HIGH COMPRESSIVE STRESS, LOW CYCLE FATIGUE OF A COMPOSITE MATERIAL

Rodney Keith Watterson

HIGH COMPRESSIVE STRESS, LOW CYCLE FATIGUE OF A COMPOSITE MATERIAL

BY

RODNEY KEITH WATTERSON

LIEUTENANT COMMANDER, UNITED STATES NAVY

B.S., UNITED STATES NAVAL ACADEMY

(1961)

SUBMITTED IN PARTIAL FULFILLMENT

OF THE REQUIREMENTS FOR THE DEGREE OF

NAVAL ENGINEER

AND THE DEGREE OF

MASTER OF SCIENCE IN NAVAL ARCHITECTURE

AND MARINE ENGINEERING

AT THE

MASSACHUSETTS INSTITUTE OF TECHNOLOGY

MAY, 1970

HIGH COMPRESSIVE STRESS, LOW CYCLE FATIGUE OF A COMPOSITE MATERIAL

BY

RODNEY KEITH WATTERSON

Submitted to the Department of Naval Architecture and Marine Engineering on May 22, 1970 in partial fulfillment of the requirements for the Master of Science degree in Naval Architecture and Marine Engineering and the Professional Degree, Naval Engineer.

ABSTRACT

The object of the work was to determine the failure mechanism associated with high uniaxial compressive stress, low cycle fatigue of a cross-ply glass fiber reinforced plastic composite material. This was followed by an investigation of the effect of misaligning a small percentage of plies within the laminate. The composite used was "Scotchply".

Specimens were cycled between a low and high compressive load in the range of 0 to 500 cycles at 6 cycles per minute. Failed and unfailed specimens were sectioned and microscopically analyzed for progressive damage.

The failure mechanism was found to originate in the plies in line with the load and appear as a progressive separation within this ply. The separation removes lateral resin support for the fibers in line with the load and local fiber buckling results.

The effect of misaligning a small percentage of plies within the laminate is to reduce the compressive fatigue strength as the misalignment angle is increased.

The work also confirmed other studies' findings concerning the effect of voids and fiber volume fraction on composite compressive strengths and a linear S-N curve for glass fiber reinforced plastics at high compressive stress and a low number of cycles. In addition, it was confirmed that a "percentage of ultimate static strength" concept does exist that permits the prediction of compressive fatigue strength of GFRP cross-ply laminates such as "Scotchply".

THESIS SUPERVISOR: JAMES W. MAR

TITLE: PROFESSOR, DEPARTMENT OF AERONAUTICS AND ASTRONAUTICS

ACKNOWLEDGMENTS

I am indebted to Professor James W. Mar, my thesis supervisor, and Dr. Larry Sheppard for their close attention to the progress of this work and many helpful suggestions.

I wish to thank Mr. Oscar Wallin and Mr. Arthur Rudolph for their assistance in the cutting and machining of the specimens and Mr. Gunther Arndt for his assistance in the polishing and microscopic examination of the tested specimens.

TABLE OF CONTENTS

LIST OF FIGURES

LIST OF TABLES

LIST OF GRAPHS

LIST OF SYMBOLS

B = Buoyancy - grams

n = Cycles

w_f = Fiber Weight Percentage

w_r = Resin Weight Percentage

w_c = Composite Weight Percentage

W_A = Composite Weight in Air - grams

W_W = Composite Weight in Water - grams

W_F = Fiber Weight - grams

W_R = Resin Weight - grams

X = Magnification

γ_f = Fiber Volume Percentage

γ_r = Resin Volume Percentage

γ_v = Void Volume Percentage

ρ_c = Composite Density (gm/cm^3) or Specific Gravity

ρ_f = Fiber Density (gm/cm^3) or Specific Gravity

ρ_r = Resin Density (gm/cm^3) or Specific Gravity

I. INTRODUCTION

Composite materials are being advertised as the answer to the excessive hull weight problems associated with deep submersibles.[12,16] The Naval Ship Research Center has been conducting hydrostatic tests on glass reinforced plastic model pressure hulls for the past ten years with impressive results.[14,15,19] This practical test program is progressing with the collection of data and performance observations and yet the actual failure mechanism of a compressive or compressive fatigue failure is not completely understood. In fact, very little work has been done in the area of compressive fatigue.

The compressive strength of a fibrous composite is directly related to the void content and shear stiffness of the matrix.[6] In addition, the compressive fatigue life of a composite is associated with compressive strength, resin content, filament orientation, macro-void content, residual stress, moisture effects, strain magnification in the matrix, glass to finish bond interface, matrix to finish bond interface, and microvoid content.[10]

This thesis is motivated with an intent to make a contribution to the understanding of the mechanism of failure associated with compressive fatigue of a fibrous reinforced composite material. Significant progress must be made in this area before full scale composite pressure hulls become a reality. In particular, this thesis will deal with high stress, low cycle fatigue of a cross-ply composite laminate. This loading and fiber arrangement is most applicable to a cylindrical submarine hull.

The composite material selected was a 3M glass reinforced plastic product. The trade name is "Scotchply" and a summary of its characteristics is given in Appendix A. The following discussion will concern the fatigue work done thus far with this product or a similar glass reinforced plastic composite.

The most extensive fatigue studies done with "Scotchply" have been by K. Boller.[1,2,3,4,5] His work has included E glass and S glass filaments and are zero mean stress fatigue studies. Boller's studies are primarily collections and displays of data with little effort made to explain the mechanism of failure. After evaluating many specimen geometries, a shortened version of the sample which Boller used for his work was chosen for this thesis.

L. J. Broutman and S. Sahu have investigated tensile fatigue of "Scotchply" in a cross-ply configuration.[7] They reported that the residual tensile strength of the fiber reinforced epoxy resin laminates subjected to fluctuating tension with a maximum stress decreases with the number of cycles. Also, they suggest a failure mechanism for tensile fatigue. It was noted that cracks develop in the material during the first cycle providing that there are fibers perpendicular to the load direction and the stress is above 20 percent of U.T.S. Cracks appear in the plies with fibers in the loading direction only when the stress level exceeds 75 percent of the U.T.S. of the material. The crack density in the plies with fibers in the loading direction first increases rapidly and then becomes constant during which time most of its life is spent. At the last stage the crack intensity in these plies increases rapidly. Hence,

it was concluded that the extent of tensile fatigue in "Scotchply" can be measured by determining the crack density in the plies with fibers in the loading direction.

The initial quickly formed cracks in the plies perpendicular to the loading direction are credited to high stress (and strain) concentrations in the resin between the fibers which are oriented at 90° to the load direction. The failure mechanism is attributed to this original cracking which then propogates into the plies with fibers parallel to the loading direction, delaminating as it progresses.

N. Fried has investigated the response of cross-ply filament wound glass reinforced composites to compressive stress.[11] He found that failure in compression tends to occur by a debonding process at the interface between perpendicular plies, in a mode which is similar to the failure mechanism in shear. In general, voids appear to control the failure process and an inverse relationship was found between shear or compressive strength as against void content. As a consequence of this, a direct linear relationship was found to exist between compressive and shear strengths. Fried also noted that in the immediate area of the break, failure is catastrophic, with considerable glass filament breakage. However, in the area somewhat removed from the break, a sharp separation at the interface was observed. This separation or debonding was noted to be remarkably similar to that observed in interlaminar shear tests of cross-ply laminates. Fried hypothesizes that compressive failure with any void content in excess of 1 percent is a debonding process and

suggests that compressive failure due to resin yield is a limiting value which can be theoretically attained but not exceeded.

J. F. Freund and M. Silvergleit[10] have surveyed the results and data of four years of compressive fatigue tests and concluded that a "percentage of ultimate" concept exists wherein the applied fatigue stress, as a percentage of true ultimate static stress can be used in reliably predicting the fatigue life of G.F.R.P. material. This percentile of true static stress appears to be a constant for any given number of cycles, irrespective of the test method, specimen fabrication or specimen geometry. This survey showed that a large amount of scatter was present for the more that 200 tests investigated. In addition, the ultimate static strength chosen as a reference for each test was at best a matter of judgment.

Based on the literature survey, a test program was set up to fabricate "Scotchply" specimens, select the best specimen shape for compressive fatigue testing, determine a reliable testing method, and develop an S-N curve concentrating on high compressive stress low cycle fatigue. Once reliable S-N data was obtained, specimens were cycled to some value less than predicted failure, sectioned, and analyzed for possible failure mechanisms. The above work was done in conjunction with another individual and used as reference data for two different theses. This thesis will compare the results of the common effort to the results obtained when a small percentage of plies are purposely misaligned in the laminate. The hypothesis is that the misaligned fibers will fail prematurely, thus initiating a total failure.

II. PROCEDURE

The composite selected for this thesis was a prepregnated plastic, reinforced with uni-directional, non-woven E-glass fiber filaments. Specifically, the material was a 3M Company product, "Scotchply" - Type 1002. The characteristics of this composite are given in Appendix A.

Fabrication

After experimenting with several different fabrication techniques, the following was considered the best:

1. Using "Scotchply" - Type 1002 tape, 12 inch square laminates were laid up of desired thickness. A 30 layer laminate was generally used. The layers were of a cross-ply configuration with adjacent layers having their fibers perpendicular. Table 1 in Appendix A contains a summary of all the laminates fabricated.
2. The laminate was wrapped in an envelope containing a releasing agent so that the laminate could be removed after the application of heat and pressure during the curing procedure.
   a. As indicated in Appendix A, some laminates were wrapped in a silicon paper, S.C.W. 33, provided by 3M specifically for this purpose.
   b. The remaining laminates were wrapped in a mylar envelope sprayed with "Frekote 33", a United Chemical product. This releasing mechanism proved superior to the silicon paper.
3. Using a hydraulic press with thermostat controlled platens the following cure cycle was used:

a. The platens were heated to 350°F and the laminates rested on the platens for five minutes.

b. The platens were closed to contact pressure and the pressure was gradually increased to 30 psi over a five minute period.

c. The pressure and temperature were maintained at 30 psi and 350°F for 10 minutes.

d. The laminate was cooled at atmospheric pressure and temperature.

This cure, with no post cure heat treatment, is advertised by 3M to produce room temperature mechanical properties of about 85 percent of those available with a 16 hour post cure at 280°F.

Specimen Geometry

The specimen dimensions are shown on Figure 1. Considerable effort was expended in arriving at this particular specimen shape. It differs from the shape tentatively recommended by A.S.T.M. for compressive testing of rigid plastics, D695-68T, but does resemble the shape chosen by those who have done compressive testing of glass reinforced plastic composites including "Scotchply". It is basically a shortened version of the specimen used by Boller in his zero mean stress fatigue testing of "Scotchply".[1]

The parallel edges of the samples were prepared on a Tensile-Kut machine and the 4 inch radius arc was cut using a milling machine.

Testing

The test program was essentially threefold. The first two parts were an effort to establish a reference standard to use as a comparison for Part 3.

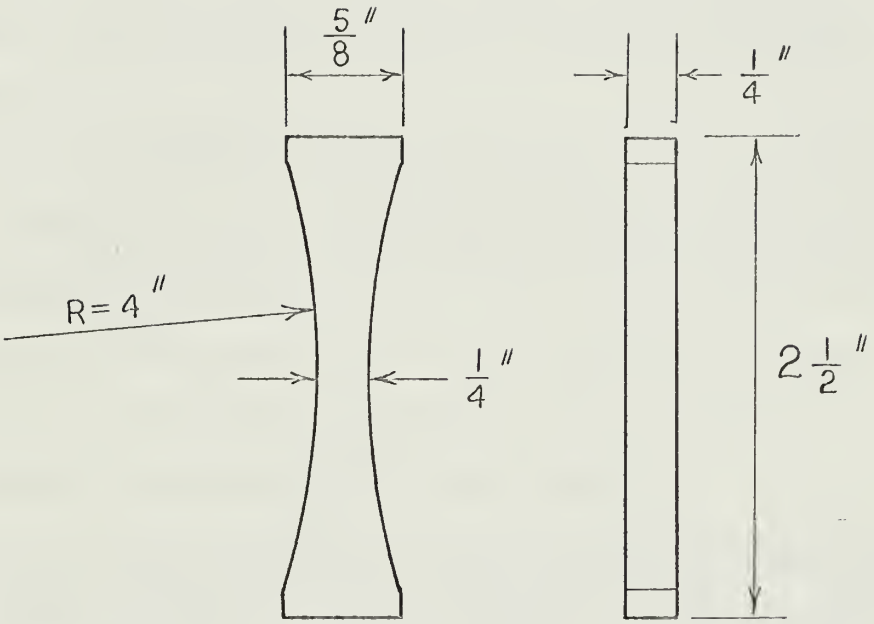

SCALE 1" = 1"

FIGURE 1 – TEST SPECIMEN

Part 1 - The first phase of the test program was to establish a high compressive stress - low cycle fatigue curve for the particular "Scotchply" and manufacturing technique used.

Part 2 - The goal of the second phase was to use the data generated in Part 1 to determine how long to cycle a series of samples at a particular stress level in order to stop short of failure and examine the samples for progressive fatigue damage.

Part 3 - This portion of the testing program was devoted to testing a series of specimens fabricated in the same manner as those for Parts 1 and 2 except that 4 plies of the laminate were purposely misaligned by 15° in one series, 30° in another and 45° in the last. The results of Part 3 were to be analyzed in comparison with Parts 1 and 2.

A picture of the testing equipment is given in Figure 2. Basically, the testing consisted of applying a cyclic compressive load at 6 cycles per minute varying between 5 percent and 75 percent to 90 percent of the expected static failure load. The test machine used was a Baldwin SR-4 compression and tension testing machine, with test load readout. As shown in the picture, the load was applied through a vertically suspended hemispheric ball joint to avoid misalignment. No end grips were used because the specimen was under a compressive loading at all times.

During testing, an aluminum restraint device was loosely fitted to the middle portion of the specimen. Originally it was felt that the restraint device should be used to insure compressive as opposed to

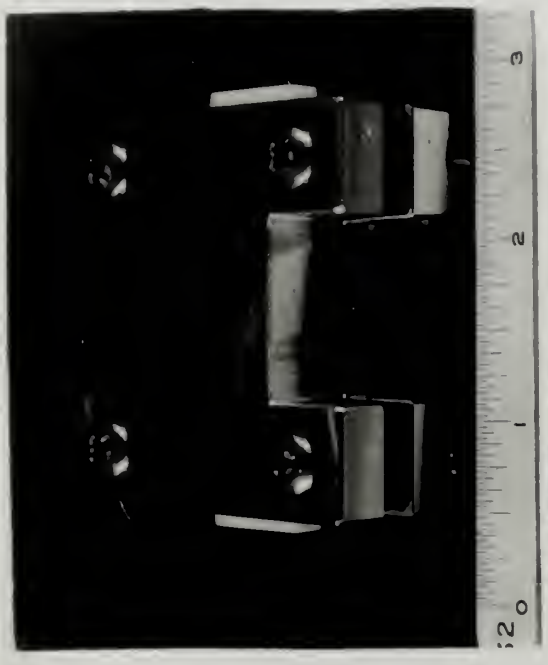

Figure 2a

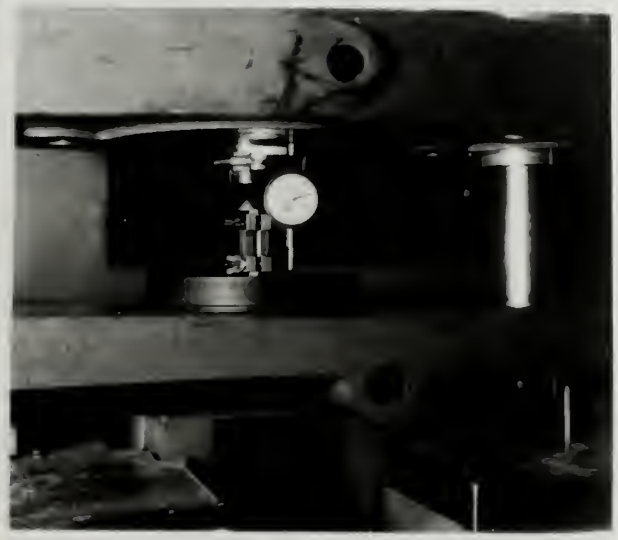

Figure 2b

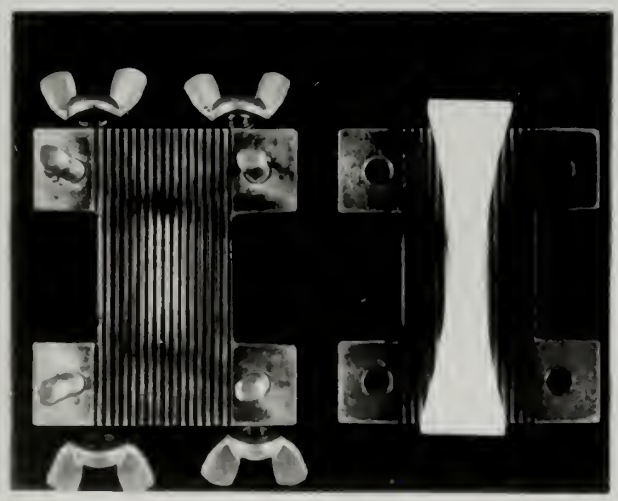

Figure 2c

Figure 2d

Restraint Device and Testing Jig

buckling failure under the high compressive loads to be used. During the testing, enough samples were tested without the restraint device to conclude that it was not really needed to insure compressive failure. The sample exhibited the same strength and type of failure with or without the restraint device. However, the most valuable contribution of the device was to reduce the severity of the failure. Without the restraint device, the failures were catastrophic, leaving very little to be microscopically analyzed. Typical failed specimens are shown in Figure 3.

Microscopic Analysis

Using the coordinate system shown in Figure 4 with the uni-direction load applied in the X direction, the following definitions are used to refer to sectioned faces of the sample:

1. Perpendicular Face - Face in YZ plane. It shows fiber ends of fibers in line with the load and fiber lengths of fibers perpendicular to the loading direction.
2. Parallel Face - Face in XZ plane. It shows fiber ends of fibers perpendicular to the load and fiber lengths of fibers in line with the load.
3. In Line Face - Face in XY plane. It shows fiber lengths of fibers in line with and perpendicular to the loading direction.

It was suspected that the progressive fatigue damage would take the form of matrix debonding, void increase in the matrix or some other mechanism associated with the deterioration of the matrix or matrix fiber interface. It was recognized that sectioning and polishing might do

Figure 3a

Figure 3b

Figure 3c

Typical Failures

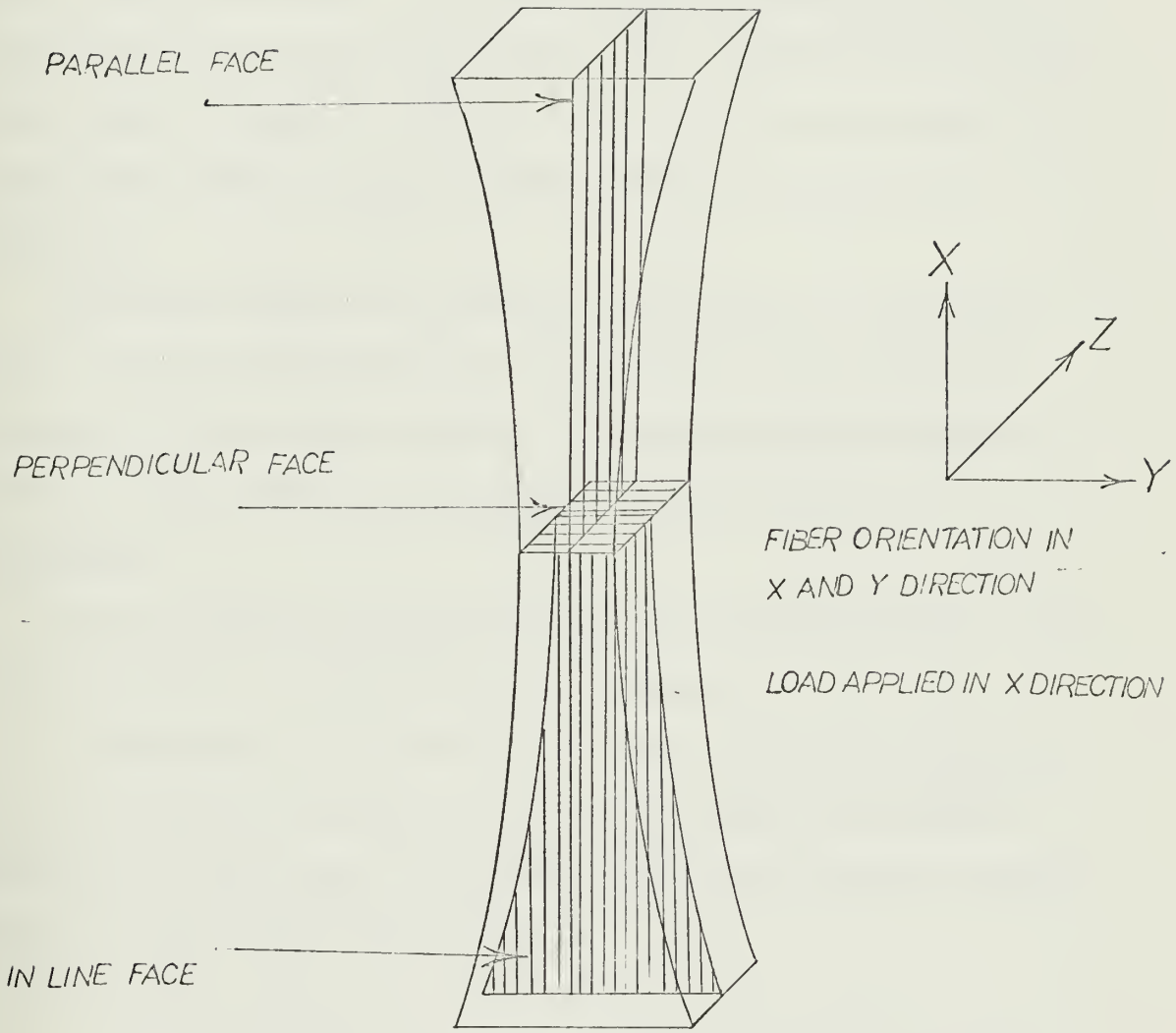

SECTIONING PLANES

FIGURE 4

damage to the matrix and give a false indication of the true damage present. When possible, post analysis was done prior to sectioning and polishing.

Sectioned samples were mounted in Quickmount and polished with paper down to 10 microns. A low speed electric polishing wheel with diamond paste was used to 1 micron and a syntron polisher with aluminum oxide powder was used to .3 microns. It was felt that the gentle, low speed syntron polisher would best avoid matrix damage during the polishing.

Microscopic analysis and photography was done on a metallograph using a Nomarski Interferemeter attachment to give the fiber detail necessary for post testing analysis. All the microscopic photographs included in this thesis were taken with the Interferemeter.

Void Content

The void content was determined for each laminate fabricated. The supporting data and calculations are in Appendix C.

A representative non tested piece of the laminate was weighed in air, then in water and finally, the resin was burned off at 630°C to determine the fiber weight. Using this data and the procedure outlined below, the void content was calculated.

ρ_c = Composite Density (gm/cm^3) or Specific Gravity

ρ_r = Resin Density (gm/cm^3) or Specific Gravity

ρ_f = Fiber Density (gm/cm^3) or Specific Gravity

W_A = Composite Weight in Air

W_W = Composite Weight in Distilled Water

B = Buoyancy = $W_A - W_W$

W_F = Weight of Fibers after Resin Burn Off

W_R = Weight of Resin = $W_A - W_F$

w_f = Fiber Weight Percentage

w_r = Resin Weight Percentage

γ_f = Fiber Volume Percentage

γ_r = Resin Volume Percentage

γ_v = Void Volume Percentage

$$\rho_c = W_A/B$$

$$w_f = W_F/W_A \times 100$$

$$w_r = W_R/W_A \times 100$$

$$\gamma_f = \frac{w_f \rho_c}{\rho_f}$$

$$\gamma_r = \frac{w_r \rho_c}{\rho_r}$$

$$\gamma_v = 100 - \gamma_f - \gamma_r$$

In theory, this method of void calculations is correct. However, there is a problem in that one must know the fiber and resin densities exactly in order to arrive at a void volume percentage of 1 or 2 percent.

The density of E-glass fibers in given as 2.54 ± 0.03 in Broutman and Krock's text.[6] However, Otto has shown that heat treating of E-glass

increases the density from 2.55 to 2.58 at 500°C.[20] Otto's data is for a 24 hour heat treatment at a specific temperature. The density change is due to compaction of the glass at elevated temperature and the density change remains when the glass is cooled to room temperature. In effect, the overnight burn off test conducted on the "Scotchply" laminates for this thesis at 630°C is a heat treatment of the glass fibers and one could expect the glass density to increase as a result of the burn off test. Based on Otto's findings, a glass density of 2.59 was chosen for purposes of void calculation for this thesis.

The density of the resin is equally as questionable. A memorandum from the 3M Company gives the density of Type 1002 resin as 1.16.[17] However, the memorandum explains that this particular resin is not ideally suited for making a resin casting and the properties of the resin casting would not necessarily be totally indicative of the properties of the resin portion of a glass reinforced laminate molded under pressure and with the resin in thin layers around and between the glass fibers. Another 3M Company reference gives the composite density as 1.84 for a resin content of 36 percent by weight.[18] Using this information and the assumed fiber density of 2.59 as shown in Appendix C, a resin density of 1.26 is arrived at. This resin density (1.26) was used for the void percentage calculations.

Considering the conflicting information available on the two densities, that must be known exactly for small void percentage calculations, it is admitted that the absolute percentages calculated for void content are debatable. However, the same densities (2.59 and 1.26) were used for all the burn off tests done at 630°C and so the relative void contents of the laminates are true indications of the relative quality of the laminates.

Appendix C contains a detailed discussion and supporting data comparing burn off tests done at 630°C and 800°C. The void percentages cited in this thesis are those calculated from 630°C burn off tests.

III. RESULTS

The results of the experiments are displayed in the form of graphs and photographs at the end of this section of the report. The supporting data for the graphs and photographs are included in Appendix B.

The following definitions are required to interpret the results:

"Failure Load" - The maximum compressive loading during the fatigue testing.

"Failure Stress" - "Failure Load"/minimum cross sectional area of the specimen

"Failure" - A sudden drop in the load of the SR-4 testing machine during the loading cycle. Always accompanied by a cracking noise.

"Number of Cycles to Failure" - Number of complete cycles between a small compressive load (approximately 5 percent of expected static failure load) and the "Failure Load".

"Ultimate Compressive Strength" - Maximum compressive strength obtained from any one specimen of a laminate.

"Misalignment Angle" - The angle between the fiber direction in the misaligned plies and the axis of the load.

Graphs

Graphs 1 through 3 present the "Failure Stress" vs "Number of Cycles to Failure" or S - N Curve for the three reference laminates. These three laminates have the following characteristics.

Laminate	Ultimate Compressive Strength	Fiber Volume Percentage	Resin Volume Percentage	Void Volume Percentage
6	70,300 psi	45.85	47.6	6.55
10	83,200 psi	58.55	39.05	2.4
11	89,000 psi	61.1	36.65	2.25

In each case the S-N curve fitting the experimental data, with the number of cycles to failure on a log scale, is best approximated by a straight line. As noted on the graphs, some tests were stopped short of failure. This was done in order to examine for progressive damage in the specimen prior to failure.

Graph 4 presents all the reference laminates nondimensionalized by dividing the "Failure Stress" of each specimen by the "Ultimate Compressive Stress" of the laminate. It too is best approximated by a straight line.

Graph 6 shows the results of the testing of specimens with misaligned fibers compared to Laminate 6. Laminates 9-15, 9-30, and 9-45 with 4 plies misaligned at 15°, 30°, and 45° respectively were compared to Laminate 6 because Laminate 6 best approximated the void volume percentages of 9-15, 9-30, and 9-45, and in addition a similar fabrication method was used for each. 9-15 shows a maximum fatigue stress of about 93 percent of the reference for an equivalent number of cycles. There is no appreciable difference between the strength reduction for the 30° misaligned plies and the 45° misaligned plies and both show a maximum fatigue stress of about 72 percent of the reference for an equivalent number of cycles. The comparisons for reduction in fatigue strength are based on the relative performance of the laminates at 30 cycles.

Graph 7 shows the results of the testing of additional specimens with misaligned fibers compared to Laminate 11. Laminates 12-30 and 13-15 with four plies misaligned at 30° and 15° respectively were compared to Laminate 11 because Laminate 11 best approximated the void volume percentages of 12-30 and 13-15 and similar fabrication methods were used for each. 13-15 shows a maximum fatigue stress of about 92 percent of the reference for an equivalent number of cycles and 12-30 shows a maximum fatigue stress of about 76 percent for an equivalent number of cycles. Again the comparisons for reduction in fatigue strength are based on the relative performance of the laminates at 30 cycles.

Graph 5 shows the percent strain vs cycles for a number of tests of the reference laminates. The strain appears to increase significantly at about 60 percent of the number of cycles to failure.

Photographs

Figure 4 shows the sectioned specimen faces defined under the microscopic analysis section in this thesis. Figures 5 through 16 show failure or progressive damage as a result of the compressive fatigue testing of reference laminates 6, 10, and 11. Figures 17 through 21 show failure damage of the laminates with misaligned plies.

Figures 5 through 16 support the following observations concerning compressive fatigue failure in cross-ply laminates.

1. The original internal damage occurs in the plies in line with the load. The damage appears as a separation within the plies and spreading of the fibers. This damage is best shown on the parallel face.

2. The damage discussed above removes the lateral support for the fibers and results in a local buckling failure of the fibers in line with the load.

3. The failure progresses through the thickness tending to debond the plies with fibers in line with the load from the cross-plies. This damage is shown best on the perpendicular face.

4. Transverse surface cracks appear early in cycling in the outer layer containing plies with fibers perpendicular to the load. Note that with an even number of layers one surface layer always has fibers perpendicular to the load direction. It was not conclusively determined that these surface cracks do or do not contribute to the initiation of complete failure.

The following guide is included to aid in interpreting photographs 5 through 16.

Figure	Above Items Supported	Laminate	Face	Notable Items
5,6,7	1	11	Parallel	Note the progressive separation in the plies in line with the load as one progresses from a nontested specimen through two stages of compressive fatigue testing.
8,9	3	11	Perpendicular	Note the separation of in line and cross-plies as failure progresses.
10,11	1	10	Parallel	These figures show the same progressive separation damage in Laminate 10 as seen in Figures 5, 6, and 7 for Laminate 11.

Figure	Above Items Supported	Laminate	Face	Notable Items
12	3	10	Perpendicular	This figure shows the same separation of in line and cross-plies in Laminate 10 as seen in Figure 9 for Laminate 11.
13		6	Parallel	Compare the excessive void content in Laminate 6 to the smaller void content in Laminates 11 and 10 shown in Figures 5 and 10 respectively.
14		11	Parallel	This photograph shows the normal appearance of the sectioned specimen after extensive cycling. There is generally little damage visible. The damage shown in Figures 5, 6, and 7 is generally not extensive.
15	4	11	In Line	This figure shows the transverse surface crack discussed above.
16	1,2,3	11	Parallel	This figure shows a failure. Note the sheared fibers and the separation of the in line and cross-plies at the left of the picture.

Figures 17 through 21 support the following observations concerning compressive fatigue failure in cross-ply laminates with misaligned plies.

1. The failure originates in the misaligned plies.
2. The major damage centers in the area of the misaligned fibers.
3. Delamination is prevalent in the misaligned fibers.

The following guide is included to aid in interpreting Figures 17 through 21.

Figure	Above Items Supported	Laminate	Face	Notable Items
17,18	2	12-30	Parallel	The failure is exaggerated in the misaligned fibers.
19	3	12-30	Perpendicular	A separation occurs between the misaligned fibers and adjacent fibers in many cases. This damage was also noticeable within the misaligned plies.
20	1	9-45	45° plane	The fiber lengths shown are the plies misaligned by 45°. These fibers have failed with little other damage noticeable outside the misaligned plies.
21	2,3	13-15 12-30		The major damage occurs in the area of the misaligned fibers. The failure travels lengthwise along the misaligned fibers or the interface between the misaligned fibers and aligned fibers.

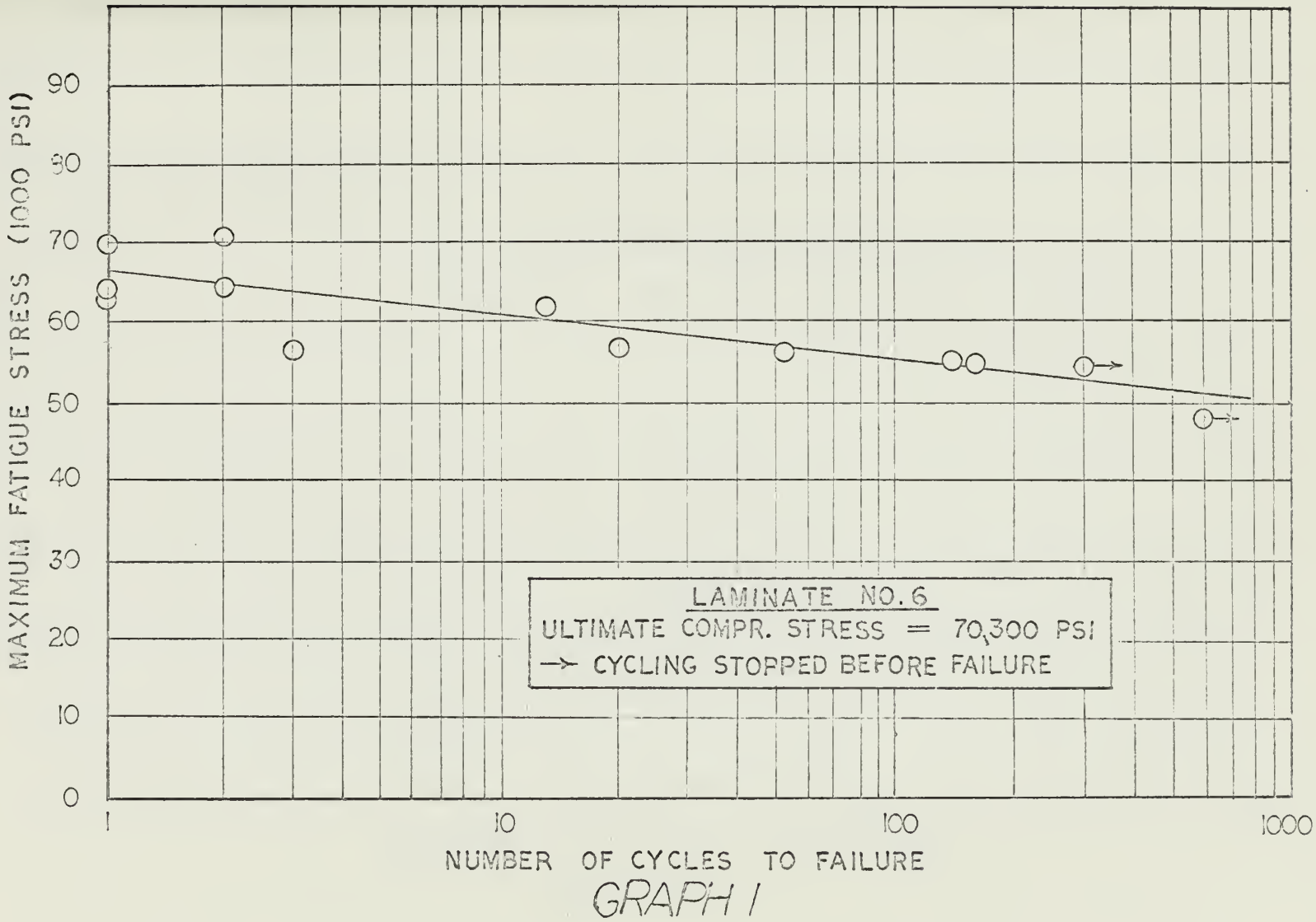
MAXIMUM FATIGUE STRESS (1000 PSI)
90
80
70
60
50
40
30
20
10
0
1
10
100
1000
NUMBER OF CYCLES TO FAILURE
LAMINATE NO. 6
ULTIMATE COMPR. STRESS = 70,300 PSI
→ CYCLING STOPPED BEFORE FAILURE

GRAPH I

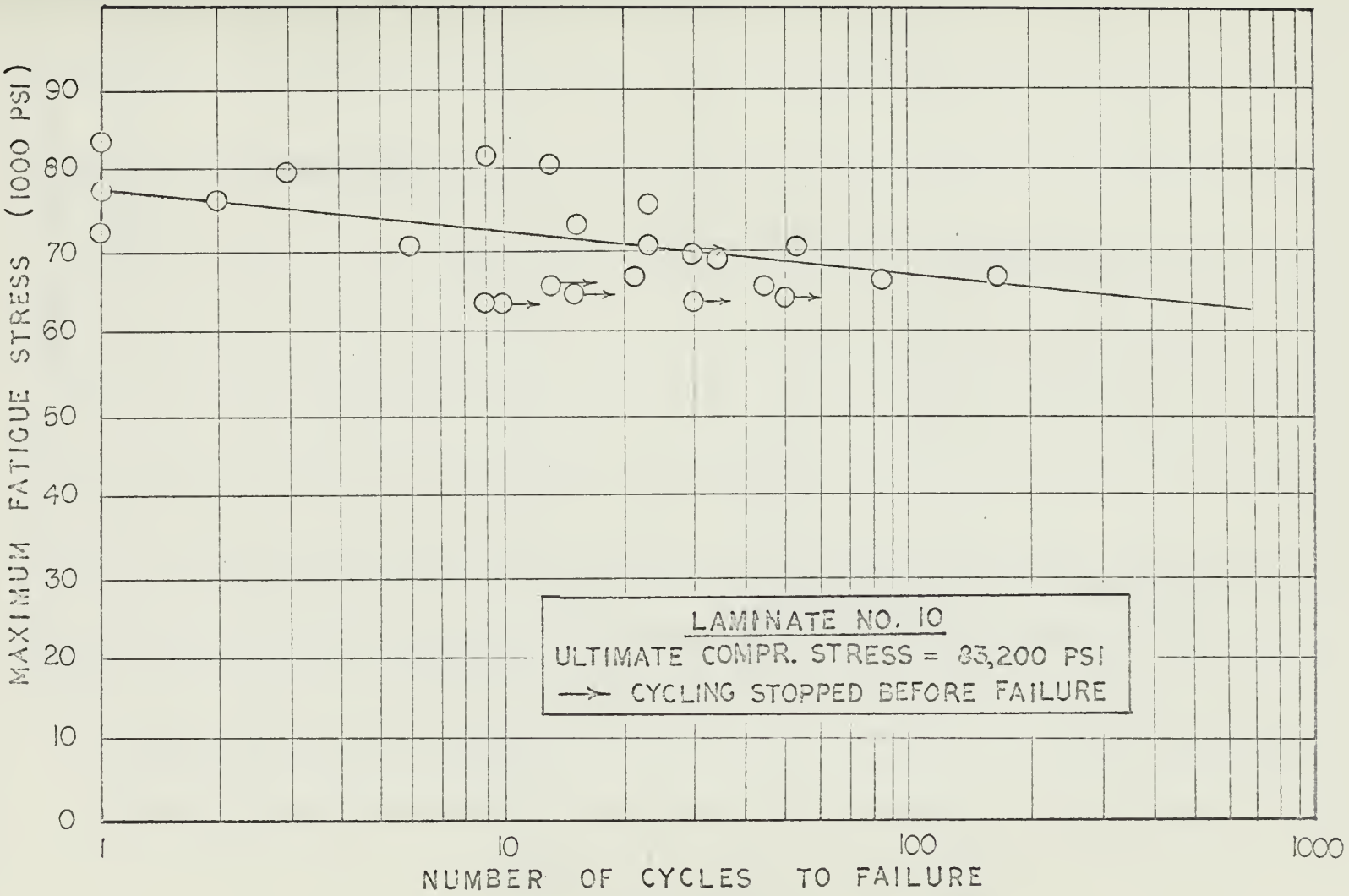
MAXIMUM FATIGUE STRESS (1000 PSI)
90
80
70
60
50
40
30
20
10
0
1
10
100
1000
NUMBER OF CYCLES TO FAILURE
LAMINATE NO. 10
ULTIMATE COMPR. STRESS = 83,200 PSI
→ CYCLING STOPPED BEFORE FAILURE

GRAPH 2

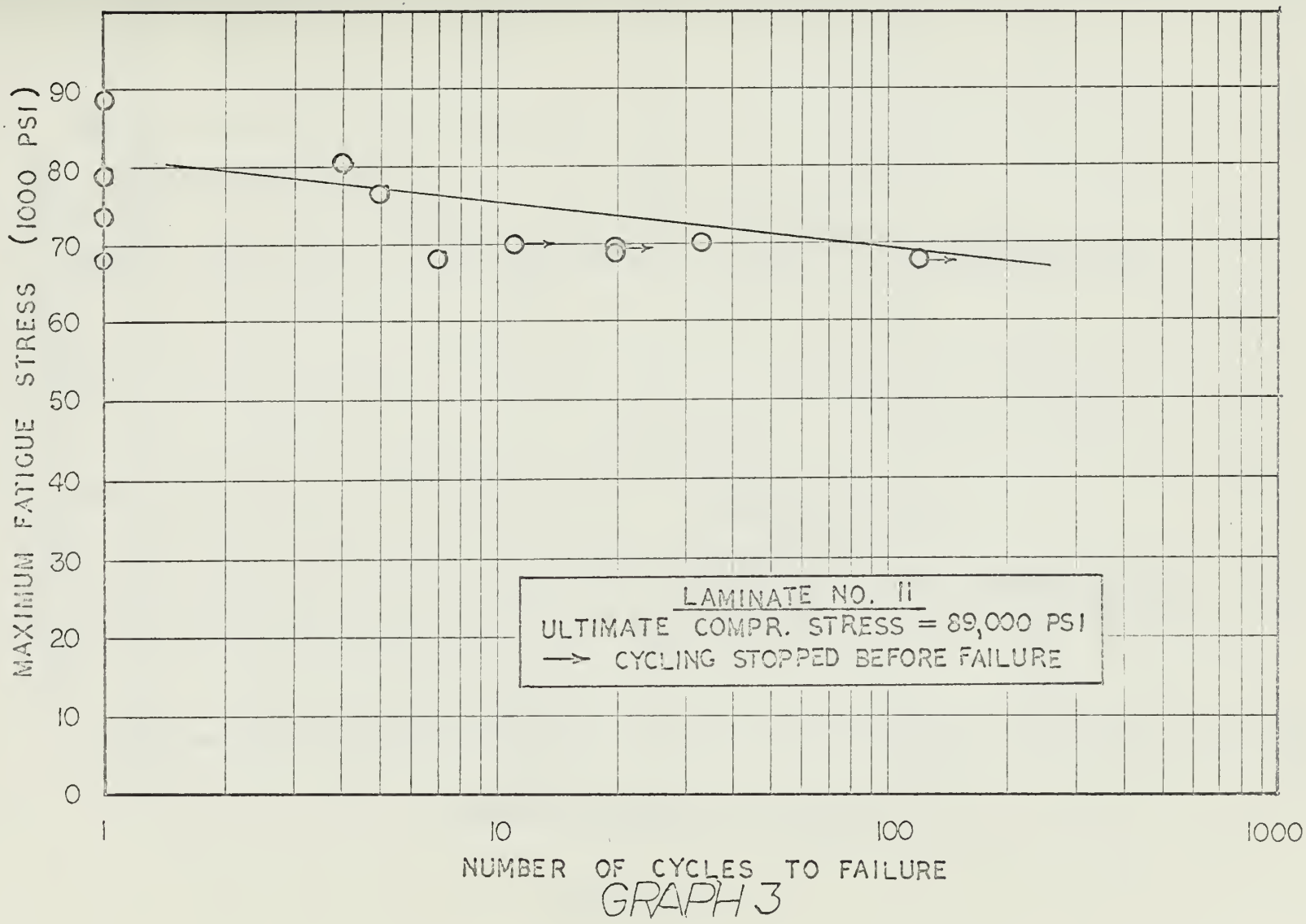
MAXIMUM FATIGUE STRESS (1000 PSI)
90
80
70
60
50
40
30
20
10
0
1
10
100
1000
NUMBER OF CYCLES TO FAILURE
LAMINATE NO. 11
ULTIMATE COMPR. STRESS = 89,000 PSI
→ CYCLING STOPPED BEFORE FAILURE

GRAPH 3

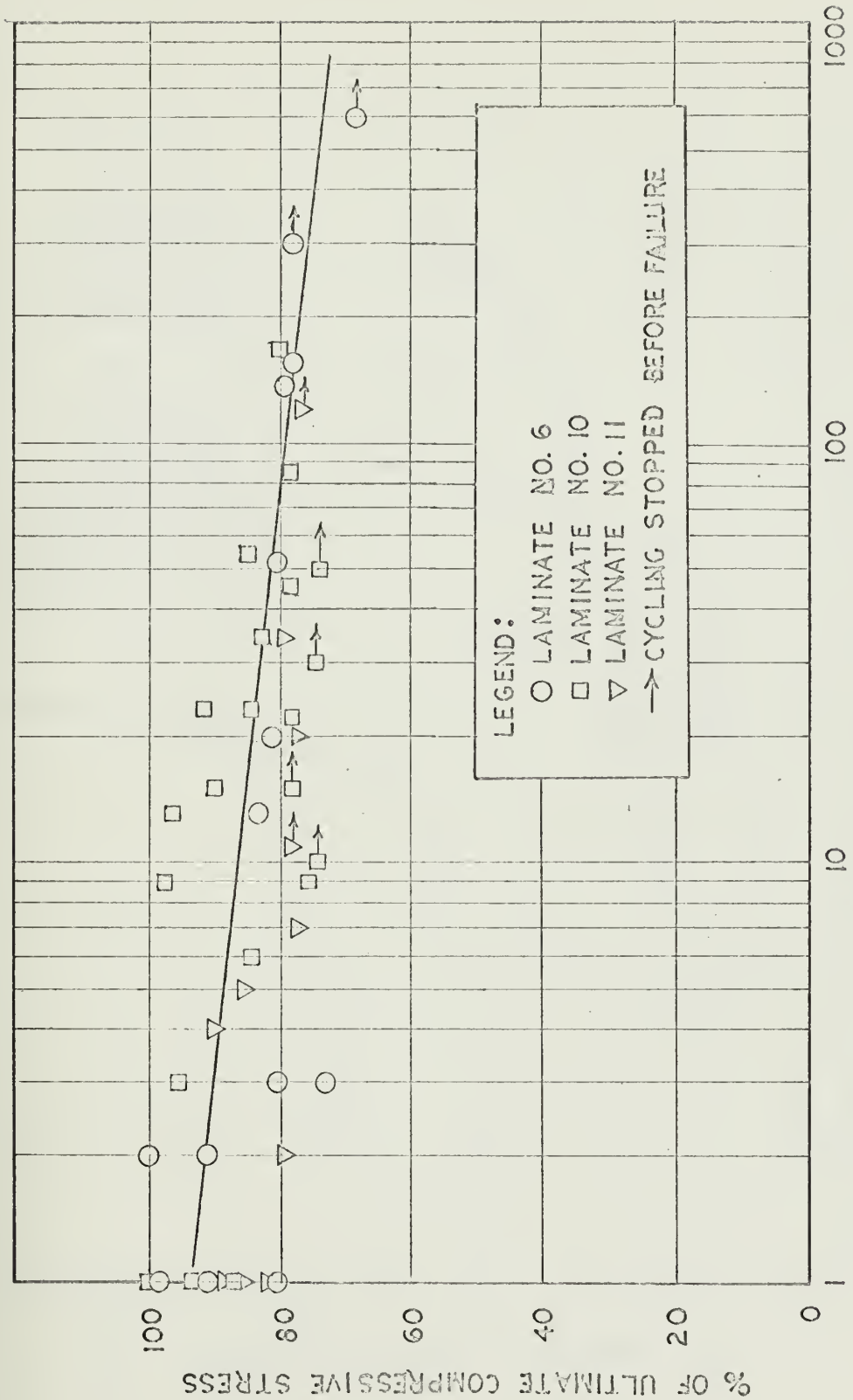
% OF ULTIMATE COMPRESSIVE STRESS
100
80
60
40
20
0
1
10
100
1000
NUMBER OF CYCLES TO FAILURE
LEGEND:
○ LAMINATE NO. 6
□ LAMINATE NO. 10
▽ LAMINATE NO. 11
→ CYCLING STOPPED BEFORE FAILURE

GRAPH 4

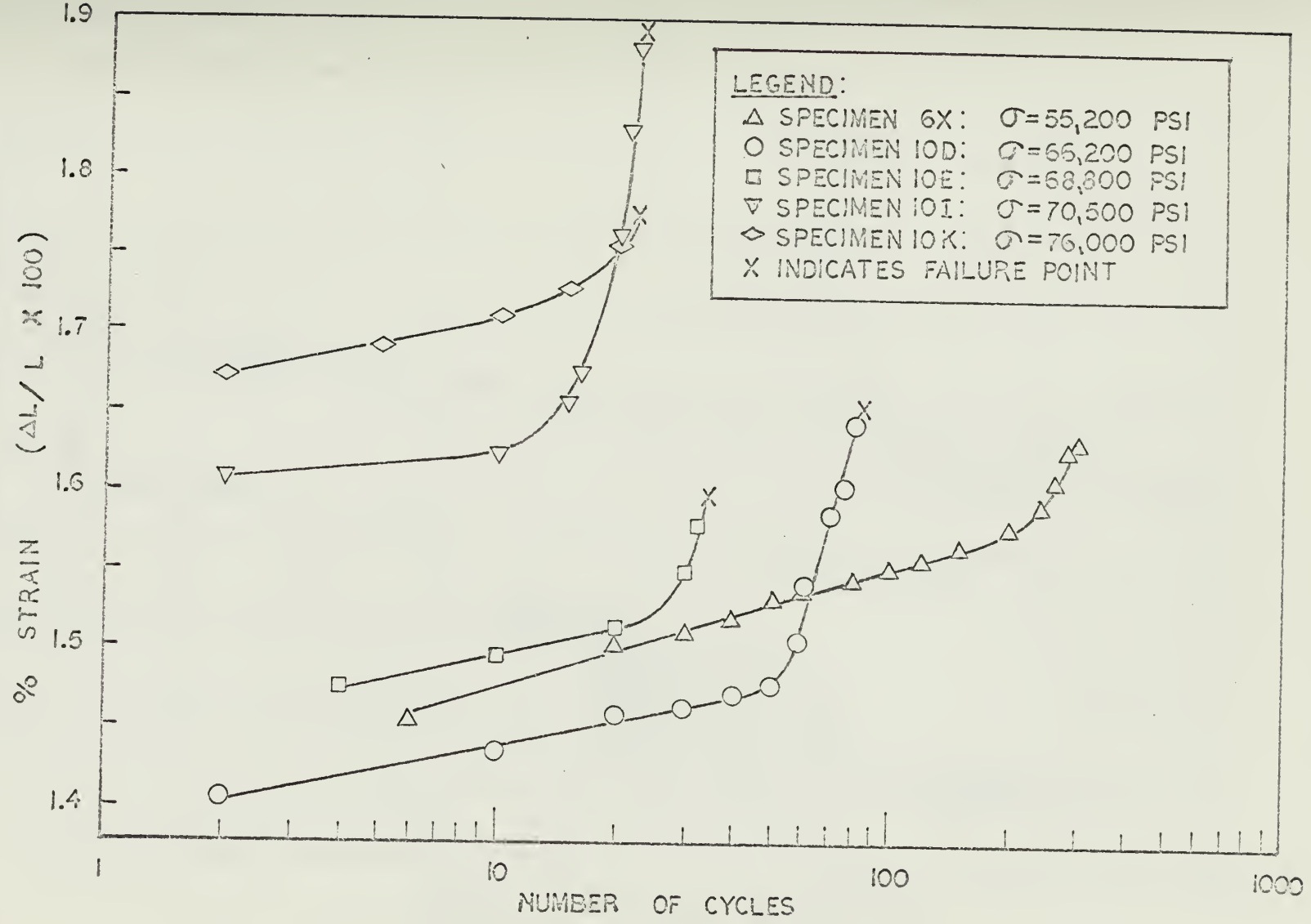
LEGEND:
SPECIMEN 6X: σ=55,200 PSI
SPECIMEN 10D: σ=66,200 PSI
SPECIMEN 10E: σ=68,800 PSI
SPECIMEN 10I: σ=70,500 PSI
SPECIMEN 10K: σ=76,000 PSI
X INDICATES FAILURE POINT
% STRAIN (ΔL/L X 100)
1.9
1.8
1.7
1.6
1.5
1.4
1
10
100
1000
NUMBER OF CYCLES

GRAPH 5

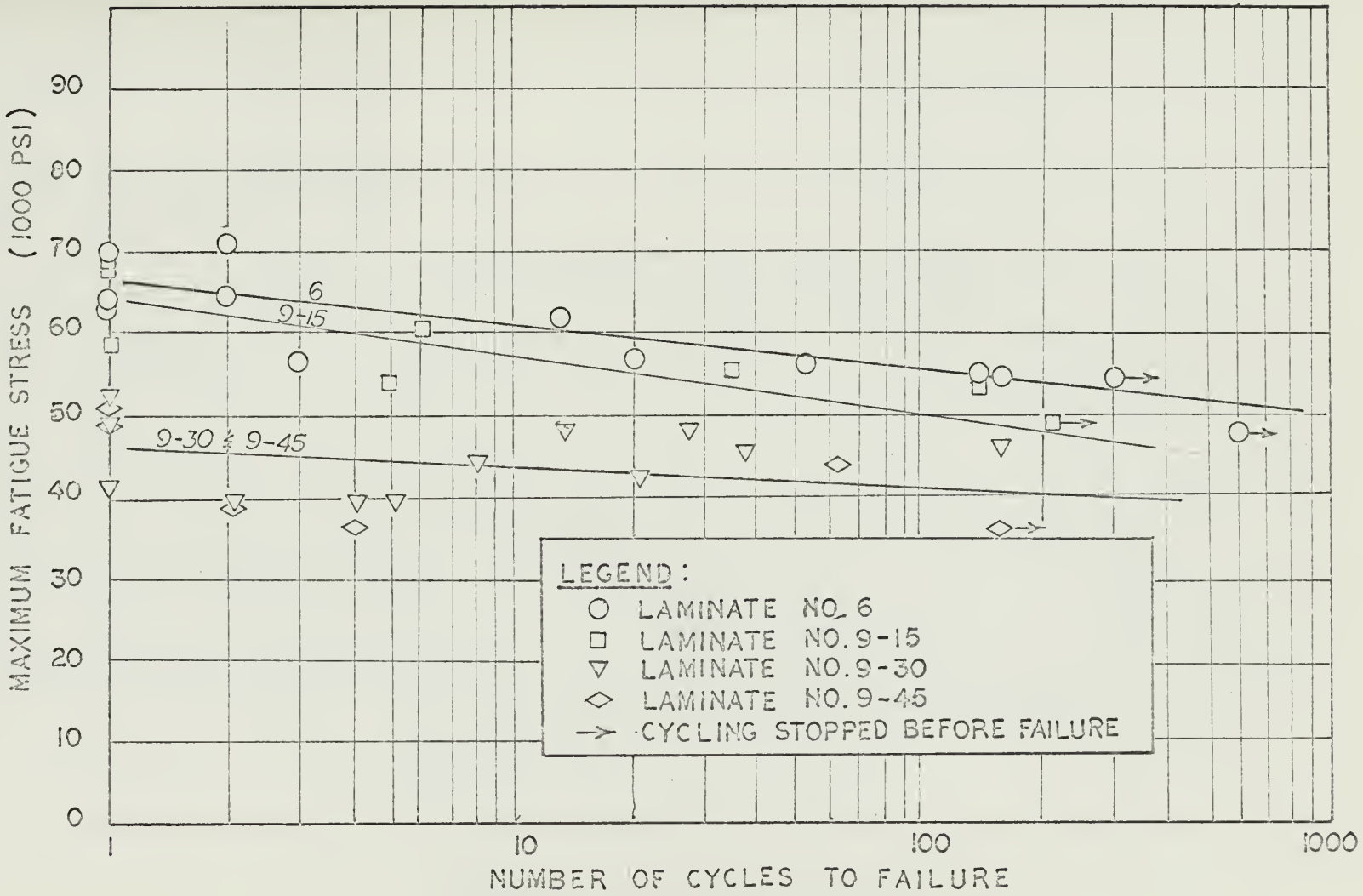
MAXIMUM FATIGUE STRESS (1000 PSI)
90
80
70
60
50
40
30
20
10
0
1
10
100
1000
NUMBER OF CYCLES TO FAILURE
6
9-15
9-30 & 9-45
LEGEND:
LAMINATE NO. 6
LAMINATE NO. 9-15
LAMINATE NO. 9-30
LAMINATE NO. 9-45
CYCLING STOPPED BEFORE FAILURE

GRAPH 6

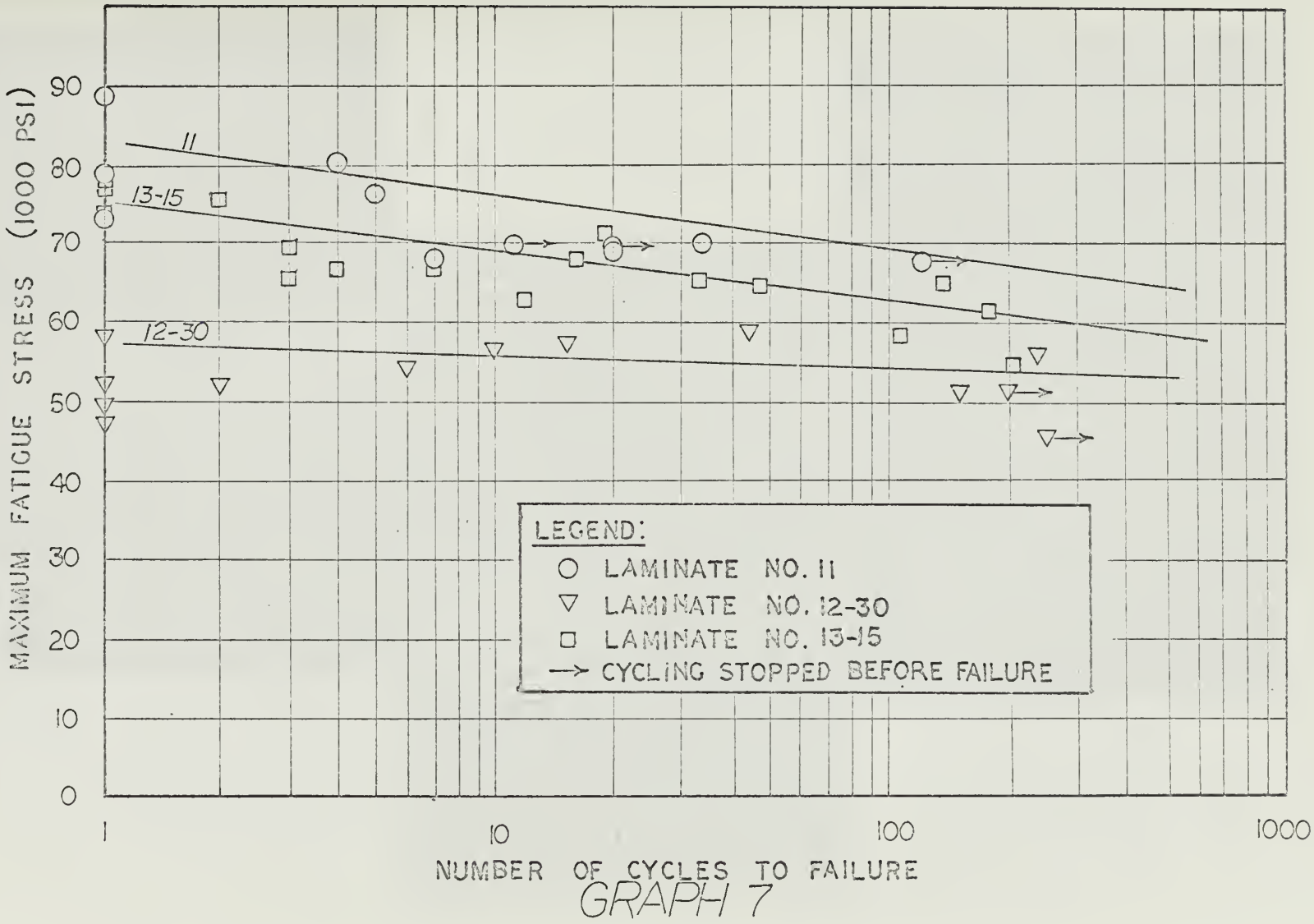
MAXIMUM FATIGUE STRESS (1000 PSI)
90
80
70
60
50
40
30
20
10
0
1
10
100
1000
NUMBER OF CYCLES TO FAILURE
11
13-15
12-30
LEGEND:
LAMINATE NO. 11
LAMINATE NO. 12-30
LAMINATE NO. 13-15
CYCLING STOPPED BEFORE FAILURE

GRAPH 7

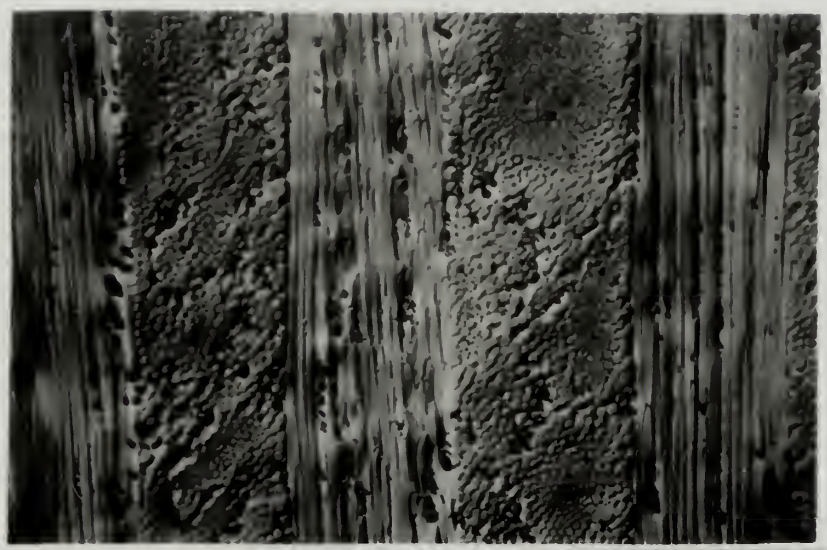

Figure 5

Laminate #11

Reference

120X

Parallel Face

Figure 6

#11 BE

69,400 psi

20 Cycles

No Failure

120X

Parallel Face

Load Direction

is Vertical

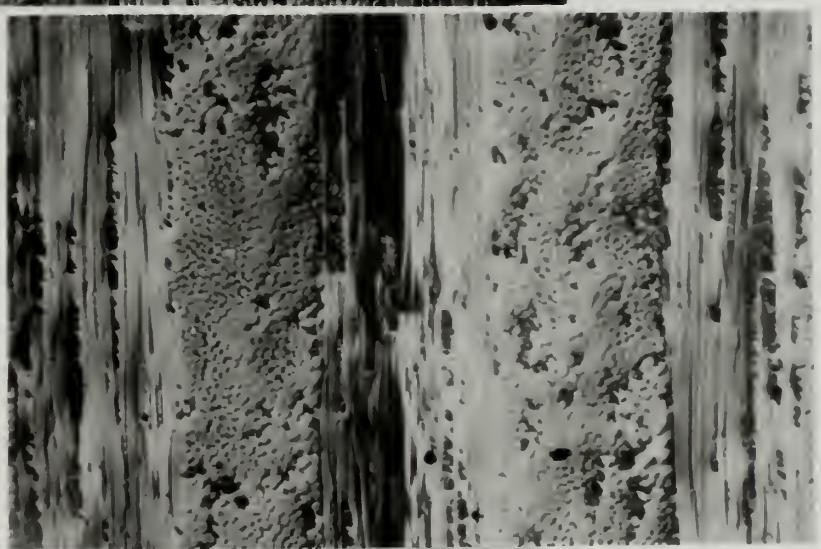

Figure 7

#11W

68,000 psi

120 Cycles

No Failure

120X

Parallel Face

Load Direction

is Vertical

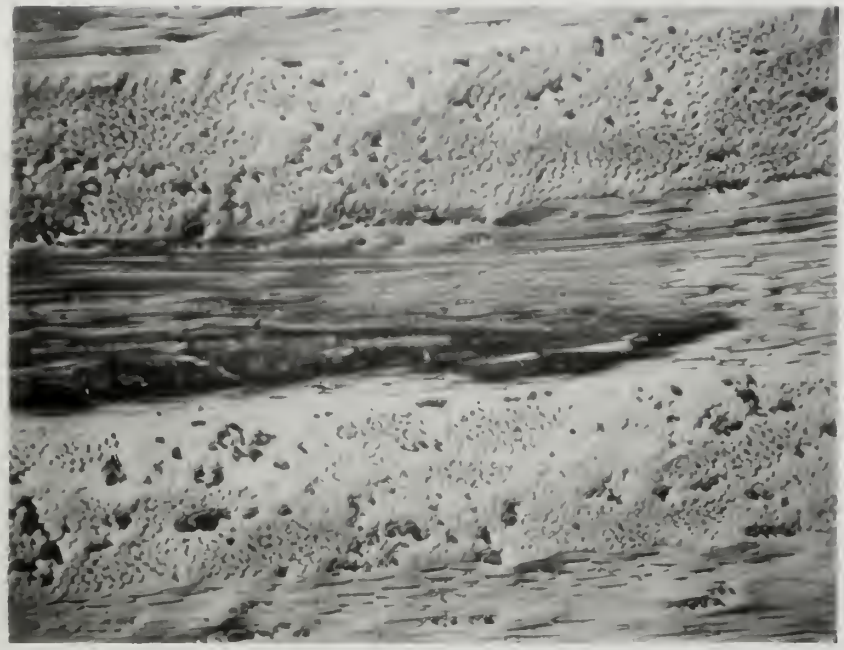

Figure 8

#11W

68,000 psi

120 Cycles

No Failure

120X

Perpendicular Face

Load Direction is

Out of the Page

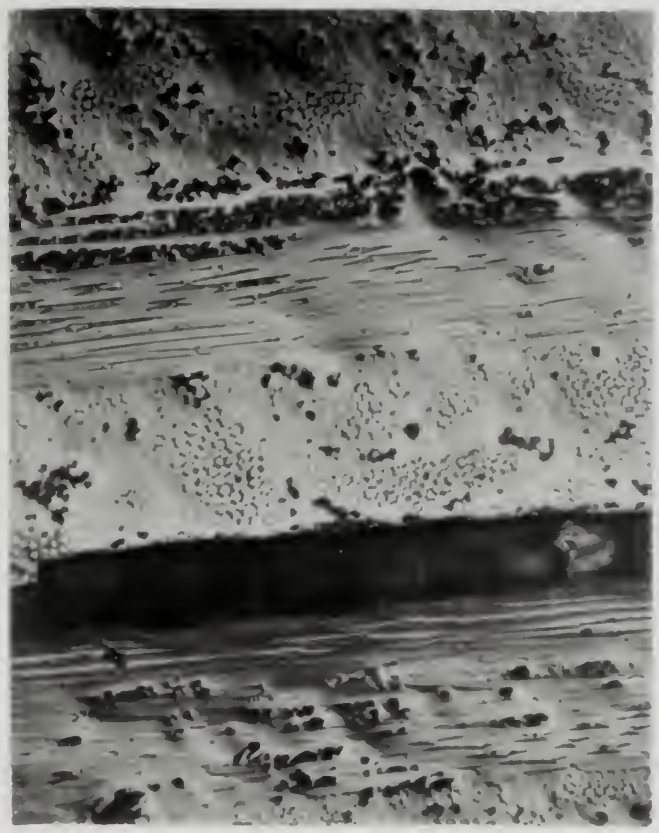

Figure 9

#11BD

61,000 psi

$\frac{1}{2}$ Cycle

Failure

120X

Perpendicular Face

Load Direction is

Out of the Page

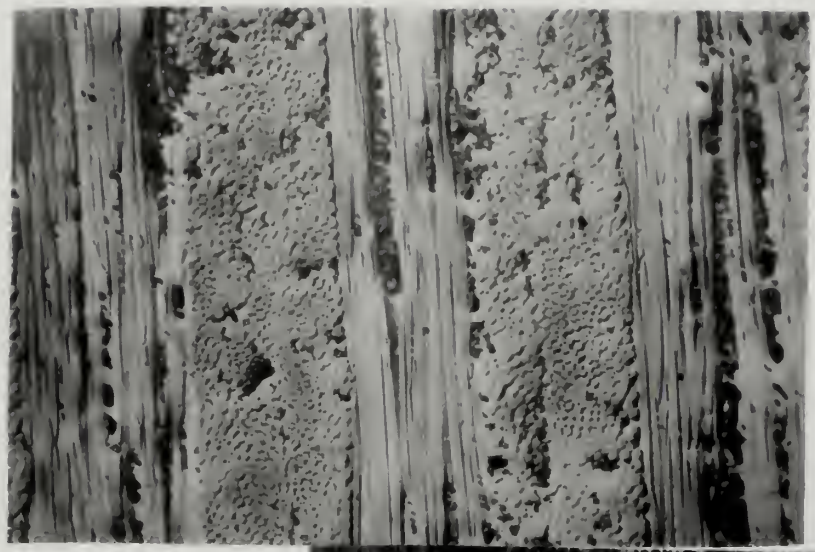

Figure 10

Laminate #10

Reference

120X

Parallel Face

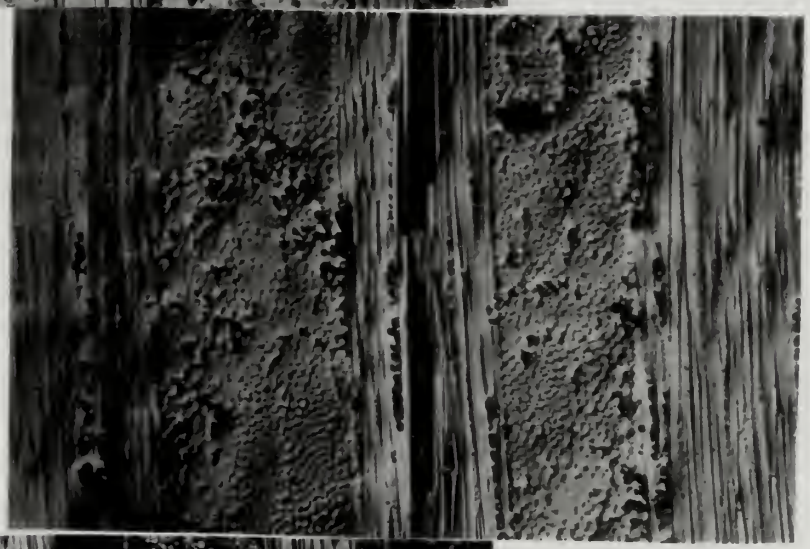

Figure 11

#10U

69,400 psi

30 Cycles

No Failure

120X

Parallel Face

Load Direction

is Vertical

Figure 12

#10N

81,000 psi

13 Cycles

Failure

120X

Perpendicular Face

Load Direction is

Out of the Page

Figure 13
Laminate #6
Reference
120X
Parallel Face

Figure 14
#11BK
70,000 psi
11 Cycles
No Failure
120X
Parallel Face
Load Direction
is Vertical

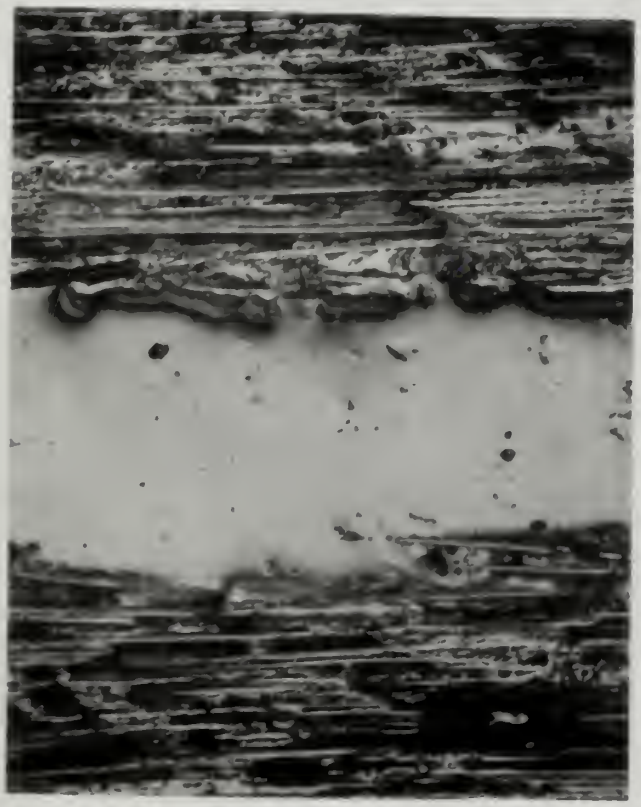

Figure 15
#11AC
67,500 psi
½ Cycle
Surface Crack
In Line Face
120X
Load Direction is
Vertical

Figure 16
#113D
61,000 psi
½ Cycle
Failure
120X
Surface Crack
Parallel Face
Load Direction
is Vertical

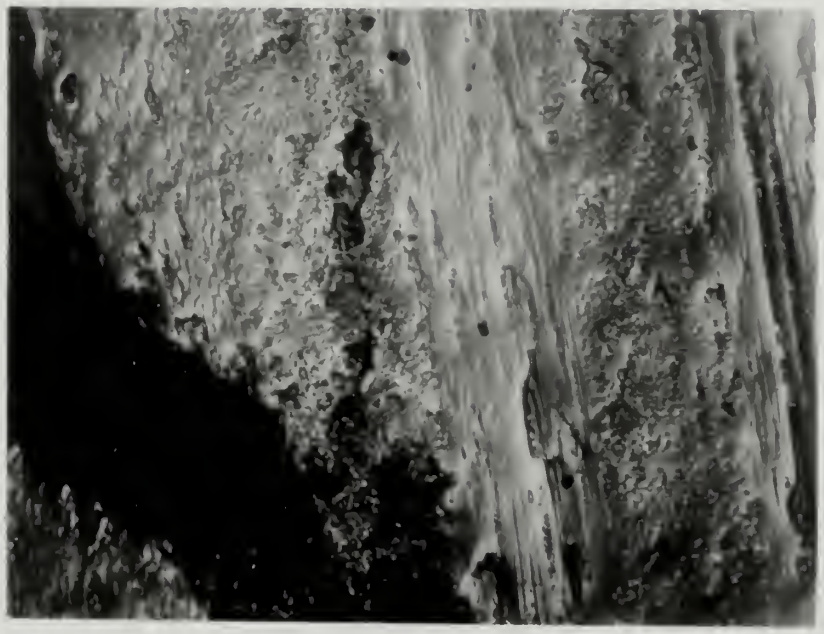

Figure 17. 12-30-I, 52,400 psi, 2 cycles, failure, 120X, parallel face, load direction is vertical, misaligned fibers on left.

Figure 18. 12-30-J, 54,600 psi, 6 cycles, failure, 120X, parallel face, load direction is vertical, misaligned fibers on left.

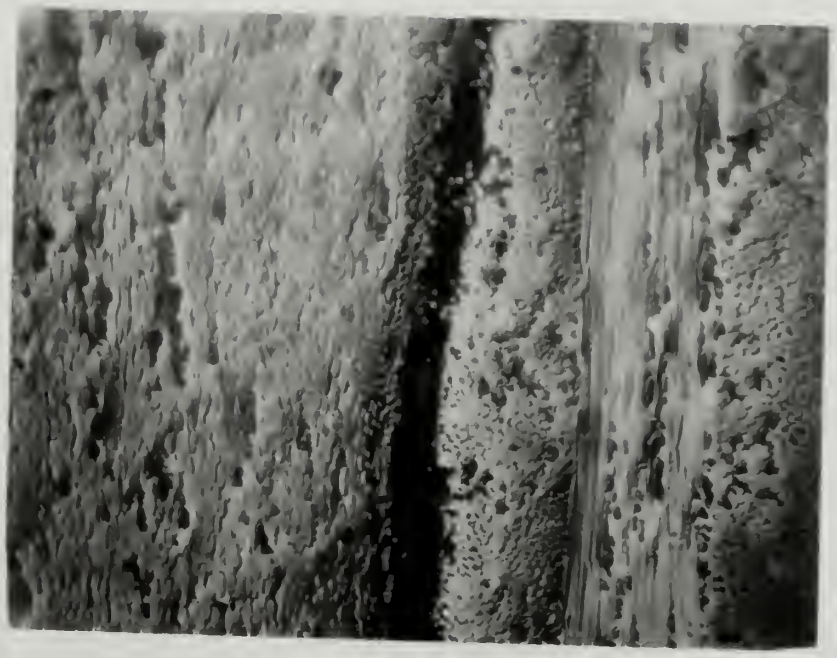

Figure 19. 12-30-I, 52,400 psi, 2 cycles, failure, 120X, perpendicular face, load direction is out of the page. Misaligned fibers on left.

Figure 20. 9-45-E, 38,300 psi, 4 cycles, failure, 120X, face shown is 45° plane through center of specimen, broken fibers are 45° misaligned fibers, fiber ends on left are vertical fibers in line with the load.

13-15-A
76,700 psi
$\frac{1}{4}$ Cycle

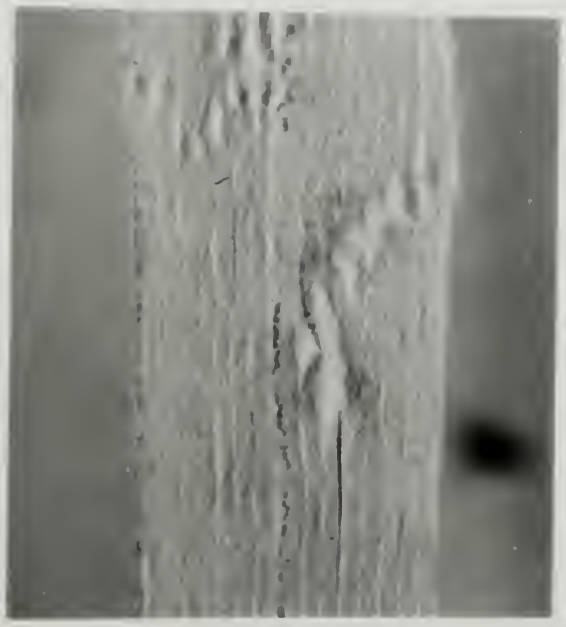

13-15-C
69,400 psi
3 Cycles

13-15-S
71,400 psi
19 Cycles

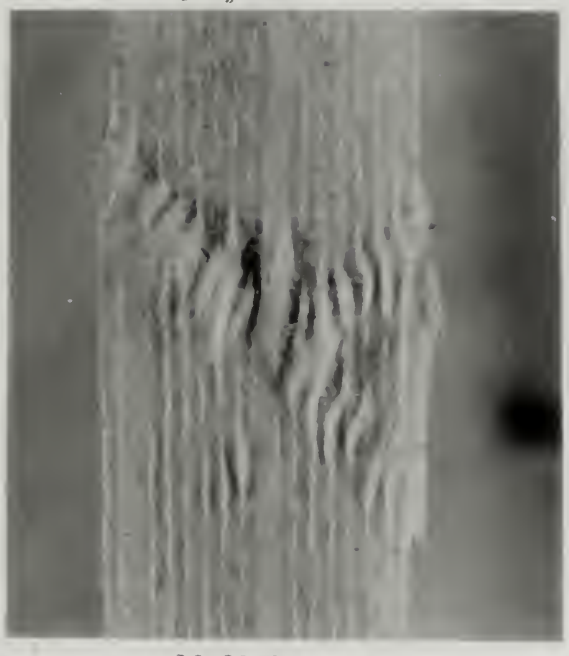

12-30-C
58,500 psi
$\frac{1}{2}$ Cycle

Figure 21. Typical Failures of Specimens with Misaligned Fibers at the Center of the Cross Section. 7X

IV. DISCUSSION OF RESULTS

Laminate Strengths

"Scotchply" - Type 1002 is advertised by 3M Company as having a compressive strength of 75,000 psi in the cross-ply configuration with the load applied in one of the fiber directions. However, with the no post cure fabrication technique used, the expected strength is 85 percent of 75,000 psi or 63,750 psi. Compare the reference laminates' fiber content and average ultimate compressive strength to that advertised by 3M.

Laminate	Fiber Weight Percentage	Void Volume Percentage	Average Ultimate Compressive Strength (Average $\frac{1}{2}$ Cycle Failures)
Advertised	64	Not Given	63,750 psi
6	66.5	6.55	65,500 psi
10	75.6	2.4	77,700 psi
11	77.4	2.25	77,100 psi

The higher fiber content and lower void content explain the higher strength of laminates 10 and 11.

Void Areas

The dark areas identified as voids on the microscopic photographs were originally suspected of possibly being dirt or polishing compound. However, numerous efforts at cleaning with a solvent and an ultrasonic cleaner and, in some cases repolishing, failed to remove or change the appearance of the dark areas. Approximately 50 specimens were sectioned, mounted, polished, and examined. The face being examined, parallel or perpendicular, could be reliably identified by observing the damage present. The progressive damage on the parallel face was consistently

within the layer of fibers in line with the load and the damage on the perpendicular face was consistently along the interface of the two normal plies.

The excessive void content in Laminate 6, shown in Figure 13, is probably due to trapped air bubbles that were not pressed out during fabrication. There was very little resin run off during fabrication as indicated by the high resin volume percentage (47.6) for this laminate.

Failure Mechanism

The failure mechanism dealing with the separation of the fibers in the plies in line with the load described in the results section of this thesis has two possible origins.

1. As described in Broutman and Krock's text, the compressive axial load causes a lateral expansion governed by poisson's ratio of the resin. Since poisson's ratio of the resin is greater than that of the glass, it expands transversely more than the glass and an interfacial tensile stress is created to preserve continuity. This local tensile stress causes debonding of the resin from the fiber and subsequent separation in the ply around the fibers.
2. The second and probably more controlling origin involves the original void distribution within the in line plies. Initial voids can be considered to be cracks which propogate according to a fracture mechanics type analysis.

The end result of both is the removal of lateral or "hydrostatic" support of the fibers in the in line plies. Local fiber buckling then results.

Figures 6, 7, and 11 show that the separation of the fibers in the plies in line with the load occurs near the center of that ply. This

appears logical in that the fibers at the extreme boundaries of the in line plies get lateral support from the cross-plies.

The proposed failure mechanism is consistent with the results obtained with the misaligned ply tests. The four adjacent layers of misaligned plies gives a large thickness without the lateral support of the cross-plies. Consequently, one would expect the separation effects to be large in the misaligned plies. Also less resin support would have to be removed from the fibers in these plies in order to cause fiber shear and failure of the composite. Figure 20 supports this hypothesis.

Figure 21 also supports the idea of failure originating in the misaligned plies. Specimen 12-30-C in particular shows both surfaces expanded indicating the failure progressed outward from the interior of the composite. Specimen 13-15-A is the only one of the four specimens shown in Figure 21 that suggests that failure did not initiate in the misaligned ply region. Considering the unpredictability of the initial void content and distribution, such a result is possible if the in line plies had a much higher initial void content than the misaligned plies. The failure appearance of Specimen 13-15-A was an exception rather than the rule.

General Failure Observations

All failures were identified by a sudden drop in load and accompanying cracking sound. As shown on Graph 5, potential failure could be identified by an increase in strain as indicated on a dial gauge graduated in .0001 inches. This knowledge was used a number of times to stop cycling short of failure in order to examine for progressive damage. The gradual increase in strain is evidence of progressive damage, perhaps separation in the in line plies, and the sharp increase in strain

is evidence of more serious damage, perhaps initial fiber breakage.

The restraint device was finger tightened and coated with graphite. Failed specimens showed graphite marks on the surface at both ends of the shear fracture indicating that the specimen had expanded most at these points. Several specimens were tested without the restraint device and they exhibited strengths comparable to others from the same laminate. However, the unrestrained specimens failed more violently with more delamination.

It is of interest to note that the half cycle failures had the same appearance as the failures that occurred after extended cycling. Both produced definite sudden failures.

Cracks appeared on the surface in the ply oriented at 90° to the load after a few number of cycles. It was suspected that these cracks might serve as failure initiators but this could not be conclusively shown. It is possible that the surface cracks reduce the support for the adjacent layer which is in line with the load permitting this layer to undergo the damage shown in Figures 6, 7, and 11.

Comparison with Other Studies

Broutman and Sahu found a systematic crack growth in the perpendicular and parallel faces as tensile fatigue progressed.[7] Compressive fatigue does not produce similar sharply defined cracks.

Fried credits compression failure in a similar material to a debonding process at the interface between perpendicular plies.[11] The process he describes appears to accompany but not initiate failure in compressive fatigue.

Fried also noted that in the immediate area of the break, failure is catastrophic, with considerable glass filament breakage. However, in

the area somewhat removed from the break, a sharp separation at an interface between adjacent plies was observed.[11] This general observation is true also for compressive fatigue. Figure 16 shows the catastrophic failure with considerable glass filament breakage and Figures 9 and 12 show the separation at a distance somewhat removed from the break.

Freund and Silvergleit concluded that a percentage of ultimate concept exists in compressive fatigue of similar materials wherein the applied fatigue stress, as a percentage of true ultimate static stress, can be used in reliably predicting the fatigue life of G.F.R.P. material.[10] Graph 4 supports this conclusion.

Freund and Silvergleit also indicate that the S-N curve for glass filament reinforced plastic materials is linear for a fatigue stress above 60 percent of ultimate uniaxial compressive stress. Graph 4 also supports this conclusion.

V. Conclusions

Compressive fatigue failure in glass fiber reinforced plastic (cross-ply) laminates is caused by a separation in the plies in line with the load that removes lateral support for the fibers in these plies. The origin of this separation is hypothesized as a fiber-resin debonding or a fracture mechanics type crack growth from initial voids.

The S-N curve for high stress compressive fatigue of glass fiber reinforced plastics (cross-ply laminates) is best approximated by a straight line up through 500 cycles.

A "percentage of ultimate static strength" concept does exist that permits the prediction of compressive fatigue strength in cross-ply laminates.

Misaligning 10 percent of the plies of a glass fiber reinforced plastic laminate (cross-ply) results in an increasing reduction of compressive fatigue strength as the misalignment angle is increased from 0° to 30°. As the misalignment angle is increased from 30° to 45°, the reduction in strength is negligible.

Burn off tests are unsatisfactory methods of determining the void or fiber content of an E-glass fiber composite. The burn off test is essentially a heat treatment that results in a permanent compaction of the glass which changes its density. A better method is to use a chemical to dissolve the matrix from the fiber.

VI. RECOMMENDATIONS

Further study in the area of compressive fatigue or cross-ply GRP laminates should include the following:

1. An investigation of laminates with and without surface plies perpendicular to the loading direction to determine the true effect of the surface cracks developed after a few cycles in the perpendicular surface plies.
2. A further investigation of the effect of misaligned fibers by misaligning only 1 or 2 plies by angles up to 30°. Failure in 1 or 2 plies may be enough to initiate failure.
3. The use of a scanning electron microscope to confirm the findings of this thesis. Despite the care taken with polishing, the possibility of damaging the sample during preparation always remains. This possibility would be reduced if a scanning electron microscope was used.
4. Fiber and void content should be determined by using a chemical to dissolve the matrix rather than burning off the matrix. The temperature required for matrix burn off changes the density of the glass.

VII. REFERENCES

1. Kenneth Boller, "Effect of Pre-cycle Stresses on Fatigue Life of Plastic Laminates Reinforced with Unwoven Fibers," Technical Documentary Report Number ML-TDR-64-168, Air Force Materials Laboratory, Wright-Patterson Air Force Base, Ohio, September, 1964.

2. Kenneth Boller, "Fatigue Characteristics of Two New Plastic Laminates Reinforced with Unwoven "S" Glass Fibers, Under Cyclic Axial or Shear Loading," Air Force Materials Laboratory, Wright-Patterson Air Force Base, Ohio, AFML-TR-66-54, May, 1966.

3. Kenneth Boller, "Effect of Single-Step Change in Stress on Fatigue Life of Plastic Laminates Reinforced with Unwoven "E" Glass Fibers," Air Force Materials Laboratory, Wright-Patterson Air Force Base, Ohio, AFML-TR-66-220, December, 1966.

4. Kenneth Boller, "Fatigue Strength of Plastic Laminates Reinforced with Unwoven "S" Glass Fibers," Air Force Materials Laboratory, Wright-Patterson Air Force Base, Ohio, AFML-TR-64-403, May, 1965.

5. Kenneth Boller and G. H. Stevens, "Effect of Type of Reinforcement on Fatigue Properties of Plastic Laminates," Wright Air Development Center, A.S.T.I.A., Document Number 213835, May, 1959.

6. L. J. Broutman and R. H. Krock, "Modern Composite Materials," Addison-Wesley Publishing Company, Reading, Massachusetts, 1967, page 101.

7. L. J. Broutman and S. Sahu, "Progressive Damage of a Glass Reinforced Plastic During Fatigue," 24th Annual Technical Conference 1969, Reinforced Plastics/Composites Division, The Society of the Plastics Industry, Inc., 1969.

8. C. K. Cole, R. H. Cornish, and J. P. Elliott, "Effect of Voids and Structural Defects on the Compressive Fatigue of Glass Reinforced Plastics," 21st Annual Meeting of the Reinforced Plastics Division,

9. Norman Davids and B. P. Gupta, "Inertial Plastic Expansion of Composite Sphears Under Explosive Loading of Cavities," Fibre Science Technology, March, 1969.

10. J. F. Freund and M. Silvergleit, "Fatigue Characteristics of Glass Reinforced Plastic Material," 21st Annual Meeting of the Reinforced Plastics Division, Section 17-B, Page 2.

11. N. Fried, "The Response of Orthogonal Filament Wound Materials to Compressive Stress," 20th Annual Meeting of Reinforced Plastics Division.

12. William R. Graner, "Reinforced Plastics for Deep-Submergence Application," Ocean Engineering, Volume 1, 1969.

13. G. S. Hollister and C. Thomas, "Fibre Reinforced Materials," American Elsevier Publishing Company, Inc., New York, New York, 1967.

14. Kenneth Hom, "Composite Materials for Pressure Hull Structures," Presented at United States Naval Applied Science Laboratory and the Polytechnic Institute of Brooklyn Symposium "Materials--Key to Effective Use of the Sea," September 12, 13, and 14, 1967.

15. Kenneth Hom et al, David Taylor Model Basin, "Investigation of Filament Reinforced Plastics for Deep-Submergence Application," A. D. 645 960, November, 1966.

16. Kenneth Hom, John E. Buhl, and Abner R. Willner, "Glass-Reinforced Plastics for Submersible Pressure Hulls," Naval Engineers Journal, Volume 75, Number 4, October, 1963.

17. Memorandum from 3M Company, Reinforced Plastics Division, St. Paul, Minnesota, concerning "Scotchply Type 1002 Resin Casting."

18. "3M Scotchply Pre-impregnated Glass Fiber Molding Materials," 3M Reinforced Plastics, Minnesota Mining and Manufacturing Company, St. Paul, Minnesota 55119.

19. N. Myers and B. Fink, "Filament Wound Structural Model Studies for Deep Submergence Vehicles," Naval Engineers Journal, Volume 77, Number 2, April, 1965.

20. William H. Otto, "Compaction Effect in Glass Fibers," American Ceramic Society Journal, Volume 44-2, February, 1961, pages 68-72.

21. "Structural Design with Fibrous Composites," The Committee on Structural Design with Fibrous Composites, Materials Advisory Board, Division of Engineering-National Research Council, Publication MAB-236, September, 1966.

22. Carl Zweben, "Comments on the Static Strength of Fiber-Reinforced Composite Materials - A Survey of the Present State of the Art," Prepared for the Fracture Panel of the NMAB AD HOC COMMITTEE ON HARDENING OF RE-ENTRY VEHICLES, March, 1969.

23. Carl Zweben, "The Strength of Notched and Damaged Composites," Mechanics Section TM 69-010, General Electric Company, Philadelphia, Pennsylvania.

VIII. APPENDIX

APPENDIX A

SUMMARY OF "SCOTCHPLY" REINFORCED PLASTIC TYPE 1002 "E" GLASS[18]

General Properties

Barcol Hardness	70
Rockwell Hardness (M) Scale	100-108
Specific Gravity	1.84
Molded Thickness (One Ply)	.010"
Water Absorption 24 Hour Immersion	.015
Wet Strength Retention (2 Hour Boil)	86%
Resin Content by Weight	36%
Maximum Operating Temperature	250°F

Mechanical Properties of Crossplied	Stress Angle 0°	45°
Flexure Strength - psi x 10^3	120	50
Modulus in Flexure - psi x 10^6	3.5	2.0
Tensile Strength - psi x 10^3	75	22
Modulus in Tensile - psi x 10^6	3.7	1.6
Compression Strength, Edge - psi x 10^3	75	23
Izoo Impact (Edgewise) - (Ft. lbs/inch notch)	35.2	59.2
Interlaminar Single Shear Strength - psi x 10^3	4.1	

TABLE 1

FABRICATION DATA SUMMARY

Laminate	Plies	Length x Width	Configuration	Releasing Agent
6	30	12" x 12"	Standard[a]	S.C.W. 33 Silicon Paper
9-15	30	6" x 6"	Standard with 4 plies misaligned at 15° [b]	S.C.W. 33 Silicon Paper
9-30	30	6" x 6"	Standard with 4 plies misaligned at 30° [b]	S.C.W. 33 Silicon Paper
9-45	30	6" x 6"	Standard with 4 plies misaligned at 45°	S.C.W. 33 Silicon Paper
10	30	12" x 12"	Standard	S.C.W. 33 Silicon Paper
11	30	12" x 12"	Standard	"Frekote" on Mylar
12-30	36	8" x 12"	Standard with 4 plies misaligned at 30° [c]	"Frekote" on Mylar
13-15	36	8" x 12"	Standard with 4 plies misaligned at 15° [c]	"Frekote" on Mylar

a Standard configuration is defined as alternating plies of 0° and 90°.

b The misaligned plies were not at the laminate center due to a fabrication error.

c The misaligned plies were located at center of the laminate.

APPENDIX B

This appendix contains the testing data for all the compressive fatigue tests. The reference laminates are covered by Tables 2 through 4 and the misaligned ply laminates are covered by Tables 5 through 9.

The reference laminates are 6, 10, and 11. The misaligned ply laminates are 9-15, 9-30, 9-45, 12-30, and 13-15, with the number after the dash indicating the angle of misalignment from the direction of the load.

All dimensions are in inches, all loads in pounds, and all stresses in psi. Cycles (n) refers to a complete cycle between a small compressive load ($\approx 5\%$ expected static failure load) and the maximum compressive load indicated as the failure load.

A + sign after a number referring to cycles indicates that the test was stopped prior to failure. A $\frac{1}{2}$ cycle failure means that the specimen failed on the initial loading cycle. These are plotted as 1 cycle failures on the S-N curve.

All tests were conducted at 6 cycles per minute.

TABLE 2

LAMINATE 6

Specimen	Width	Thickness	Failure Load	Failure Stress	Cycles
6H	.283	.254	4980	69,500	½
6J	.280	.253	4980	70,300	2
6K	.294	.263	5000	64,600	2
6L	.286	.261	4100	55,000	154
6M	.288	.263	4850	64,000	½
6N	.293	.264	4800	62,000	13
60	.289	.253	4600	62,900	½
6Q	.277	.258	4050	56,700	3
6S	.292	.252	4100	55,600	136
6V	.285	.253	3460	47,900	600+
6W	.277	.256	4100	56,900	20
6X	.290	.256	4100	55,200	300+
6Y	.278	.250	3920	56,400	52

STRAIN DATA FOR 6X Length = 2.542

n	ΔL	ΔL/L x 100
6	.0370	1.455
20	.0382	1.500
30	.0384	1.510
40	.0387	1.525
50	.0390	1.535
60	.0391	1.540
80	.0393	1.545

STRAIN DATA FOR 6X (Continued)

n	ΔL	$\Delta L/L \times 100$
90	.0395	1.555
100	.0395	1.555
110	.0396	1.560
120	.0396	1.560
130	.0398	1.570
150	.0399	1.570
160	.0401	1.580
190	.0402	1.580
200	.0402	1.580
210	.0405	1.590
240	.0405	1.590
260	.0409	1.610
280	.0414	1.630
300	.0415	1.630

TABLE 3

LAMINATE 10

Specimen	Width	Thickness	Failure Load	Failure Stress	Cycles
10A	.273	.226	5140	83,200	½
10B	.292	.220	4200	65,300	45
10C	.295	.226	4220	63,200	9
10D	.291	.225	4320	66,200	84
10E	.291	.224	4450	68,800	34
10F	.286	.222	4500	70,700	54
10G	.287	.222	4220	66,200	22
10H	.276	.223	4320	70,500	6
10I	.285	.225	4520	70,500	23
10J	.250	.227	4190	73,800	15
10K	.271	.224	4620	76,000	23
10L	.250	.222	4010	72,400	½
10M	.272	.223	4850	79,700	3
10N	.269	.226	4920	81,000	13
10O	.250	.230	4380	76,300	2
10P	.287	.223	4250	66,500	167
10Q	.272	.221	4650	77,500	½
10S	.272	.225	4950	81,800	9
10Z	.256	.214	3400	62,000	30+
10U	.257	.215	3600	69,400	30+

Specimen	Width	Thickness	Failure Load	Failure Stress	Cycles
10AA	.236	.207	3180	65,000	15+
10AB	.256	.208	3490	65,400	13+
10AF	.265	.214	3500	61,900	10+
10AG	.247	.213	3280	62,600	50+

STRAIN DATA FOR LAMINATE 10

10D Length = 2.493

n	ΔL	ΔL/Lx100
2	.0350	1.410
10	.0358	1.440
20	.0364	1.460
30	.0365	1.465
40	.0367	1.475
50	.0369	1.485
58	.0376	1.510
60	.0385	1.550
70	.0396	1.590
75	.0400	1.605
78	.0406	1.630
80	.0410	1.645
84	.0412	1.655

10E Length = 2.495

n	ΔL	ΔL/Lx100
4	.0368	1.475
10	.0373	1.495
20	.0378	1.515
30	.0387	1.550
32	.0394	1.580
34	.0398	1.595

STRAIN DATA FOR LAMINATE 10 (Continued)

10I	Length = 2.494		10K	Length = 2.496	
n	$\triangle L$	$\triangle L/L \times 100$	n	$\triangle L$	$\triangle L/L \times 100$
1	.0392	1.575	2	.0417	1.675
2	.0400	1.610	5	.0422	1.690
10	.0405	1.630	10	.0426	1.710
15	.0412	1.650	15	.0431	1.730
16	.0418	1.680	20	.0438	1.760
20	.0440	1.765			
21	.0457	1.835			
22	.0469	1.885			
23	.0473	1.900			

TABLE 4

LAMINATE 11

Specimen	Width	Thickness	Failure Load	Failure Stress	Cycles
11A	.256	.233	5300	89,000	½
11W	.257	.235	4100	68,000	120+
11Y	.256	.235	4220	70,000	34
11Z	.257	.235	4160	68,900	7
11AA	.255	.230	4700	80,200	4
11AB	.263	.238	4760	76,100	5
11AD	.258	.240	4260	69,000	20
11BA	.262	.231	4760	79,000	½
11BC	.262	.226	4320	73,000	½
11BE	.266	.227	4200	69,400	20 +
11AC	.255	.237	4060	67,500	½
11BD	.262	.233	3720	61,000	½
11BK	.258	.227	4100	70,000	11

TABLE 5

LAMINATE 9-15

Specimen	Width	Thickness	Failure Load	Failure Stress	Cycles
9-15-A	.260	.217	3800	67,400	½
9-15-B	.262	.214	3400	60,600	6
9-15-C	.256	.200	2780	54,500	5
9-15-F	.257	.202	2900	55,900	33
9-15-H	.262	.201	2800	53,200	134
9-15-J	.244	.204	2440	48,800	200+
9-15-K	.254	.214	3200	58,900	½
9-15-L	.258	.203	3590	68,500	½

TABLE 6

LAMINATE 9-30

Specimen	Width	Thickness	Failure Load	Failure Stress	Cycles
9-30-A	.269	.215	2840	49,200	½
9-30-B	.270	.158	2050	48,000	26
9-30-C	.264	.211	2540	45,600	150
9-30-D	.275	.203	2200	39,500	4
9-30-E	.264	.186	1960	39,900	5
9-30-F	.263	.198	2140	40,800	½
9-30-G	.267	.177	2460	52,100	½
9-30-H	.273	.202	2200	40,000	2
9-30-I	.265	.195	2200	42,500	20
9-30-J	.269	.206	2660	48,000	13
9-30-K	.260	.210	2420	44,400	8
9-30-L	.268	.214	2600	45,300	36

TABLE 7

LAMINATE 9-45

Specimen	Width	Thickness	Failure Load	Failure Stress	Cycles
9-45-A	.260	.198	2040	39,700	2
9-45-C	.257	.203	1800	34,500	150+
9-45-D	.259	.196	2550	50,700	½
9-45-E	.267	.203	2170	38,300	4
9-45-F	.262	.203	2600	48,900	½
9-45-G	.260	.197	2250	44,000	59

TABLE 8

LAMINATE 12-30

Specimen	Width	Thickness	Failure Load	Failure Stress	Cycles
12-30-A	.255	.299	2650	45,400	250+
12-30-B	.253	.222	3300	58,900	44
12-30-C	.251	.226	3310	58,500	½
12-30-D	.253	.233	3400	57,600	15
12-30-F	.254	.227	3180	56,100	236
12-30-G	.251	.226	2680	47,500	½
12-30-H	.245	.227	2900	52,200	½
12-30-I	.223	.257	3000	52,400	2
12-30-J	.227	.258	3200	54,600	6
12-30-K	.230	.254	3000	51,400	200+
12-30-L	.228	.255	3350	58,100	½
12-30-M	.225	.252	3060	54,000	6
12-30-N	.220	.255	2800	49,900	½
12-30-O	.221	.253	3200	57,300	10
12-30-P	.231	.252	3000	51,600	151

TABLE 9

LAMINATE 13-15

Specimen	Width	Thickness	Failure Load	Failure Stress	Cycles
13-15-A	.261	.233	4660	76,700	½
13-15-B	.260	.230	4360	73,000	½
13-15-C	.270	.226	4220	69,400	3
13-15-E	.266	.232	4200	68,000	16
13-15-H	.258	.231	3480	58,600	107
13-15-I	.258	.233	3700	61,500	181
13-15-J	.253	.236	3740	62,700	12
13-15-K	.254	.236	3900	65,200	138
13-15-L	.256	.239	4100	67,000	7
13-15-N	.252	.239	3900	64,700	47
13-15-O	.252	.242	4000	65,600	3
13-15-P	.248	.242	4000	66,700	33
13-15-Q	.252	.230	4520	77,800	½
13-15-R	.257	.221	3800	66,900	4
13-15-S	.252	.239	4300	71,400	19
13-15-T	.252	.242	4580	75,200	2
13-15-U	.251	.226	3200	56,400	205

APPENDIX C

CALCULATION OF VOID CONTENT

Determination of the Resin Density

Information supplied by 3M:[18]

$$\rho_c = 1.84$$

$$w_r = .36$$

$$w_f = .64$$

$$w_c = 1.00$$

Based on Otto's findings:[20]

$$\rho_f = 2.59$$

Assuming 3M's sample had no voids:

$$\frac{w_f}{\rho_f} + \frac{w_r}{\rho_r} = \frac{w_c}{\rho_c}$$

$$\frac{.64}{2.59} + \frac{.36}{\rho_r} = \frac{1}{1.84}$$

$$= \rho_r = 1.26$$

Burn Off Tests at 800°C

The first burn off tests were done at 800°C overnight with unsatisfactory results. Instead of individual white fibers remaining after the resin had burned off, the glass appeared to have fused together and was black in color. It was determined that 800°C was not needed and in fact the oven temperature was probably higher than 800°C because of an oven malfunction. A fiber density of 2.61 was assumed for these tests and the results are given in Tables 12, 13, and 14 of this Appendix. This

data is considered questionable but is included because it tends to support that data obtained in the final burn off tests at 630°C.

Burn Off Tests at 630°C.

The burn off tests done at 630°C resulted in individual white fibers remaining after burn off. The tests were conducted overnight and then the fibers were heated for several hours again the next day to insure there was no additional weight drop in the fiber weight. The results of these tests are given in Tables 10, 11, and 14 of this Appendix. An assumed fiber density of 2.59 was used. This data is considered the most reliable and consequently the figures for this test are used in the main body of the thesis.

Comparison of Both Tests.

A summary of the results of both tests are given in Table 14. The results compare favorably with the exception of the 9 laminates. It must be reemphasized that the calculations for void content are strongly influenced by the assumed densities of the fiber and resin. The void contents calculated give a good relative indication of the quality of the laminates used in this thesis but may not be good absolute values.

TABLE 10

CALCULATIONS FOR VOID CONTENT

REFERENCE LAMINATES

All Weights in Grams
Burn Off Temperature = 630°C (1168°F)

Fiber Density = 2.59
Resin Density = 1.26

	Laminate			6	6	10	10	11	11
1	Reference	Includes Aluminum Wire		.0242	.0242	.0212	.0242	.0245	.0235
2	Dry Weight	Includes (1)	W_D	.4246	.5909	.5168	.8081	.1461	.5321
3	Wet Weight	Includes (1)	W_W	.2056	.2650	.2674	.4227	.0868	.2824
4	Buoyancy	(2)-(3)	B	.2190	.3259	.2494	.3854	.0593	.2497
5	Weight in Air	(2)-(1)	W_A	.4004	.5667	.4956	.7839	.1216	.5086
6	Composite Density	(5)/(4)	ρ_c	1.83	1.742	1.99	2.03	2.05	2.04
7	Fiber Weight	After Burn Off	W_F	.2644	.3785	.3716	.5976	.0941	.3942
8	Resin Weight	(5)-(7)	W_R	.1360	.1882	.1240	.1863	.0275	.1144
9	Fiber Weight %	(7)/(5)x100	w_f	66.1	66.8	74.9	76.2	77.4	77.5
10	Resin Weight %	(8)/(5)x100	w_r	33.9	33.2	25.1	23.8	22.6	22.5
11	Fiber Volume %	(9)(6)/2.59	γ_f	46.7	45.0	57.5	59.6	61.2	61.0
12	Resin Volume	(10)(6)/1.26	γ_r	49.3	45.9	39.7	38.4	36.8	36.5
13	Void Volume %	100-(11)-(12)	γ_v	4.0	9.1	2.8	2.0	2.0	2.5

TABLE 11

CALCULATIONS FOR VOID CONTENT

MISALIGNED PLY LAMINATES

All Weights in Grams
Burn Off Temperature = 630°C (1168°F)

Fiber Density = 2.59
Resin Density = 1.26

	Laminate			9-15	9-15	9-30	9-30	9-30
1	Reference	Includes Aluminum Wire		.0242	.0239	.0204	.0223	.0239
2	Dry Weight	Includes (1)	W_D	.4120	.3474	.4169	.4504	.3377
3	Wet Weight	Includes (1)	W_W	.2130	.1877	.2230	.2423	.1827
4	Buoyancy	(2)-(3)	B	.1990	.1597	.1939	.2081	.1550
5	Weight in Air	(2)-(1)	W_A	.3878	.3235	.3965	.4281	.3138
6	Composite Density	(5)/(4)	ρ_c	1.945	2.025	2.05	2.055	2.012
7	Fiber Weight	After Burn Off	W_F	.2928	.2478	.3134	.3430	.2473
8	Resin Weight	(5)-(7)	W_R	.0950	.0757	.0831	.0851	.0665
9	Fiber Weight %	(7)/(5) x100	w_f	.756	.766	.791	.802	.788
10	Resin Weight%	(8)/(5) x100	w_r	.244	.234	.209	.198	.212
11	Fiber Volume %	(9)(6)/2.59	γ_f	56.8	59.2	62.6	63.5	61.1
12	Resin Volume %	(10)(6)/1.26	γ_r	37.6	37.6	33.9	32.3	33.8
13	Void Volume %	100-(11)-(12)	γ_v	5.6	3.2	8.5	4.2	5.1

TABLE 11 (CONTINUED)

CALCULATIONS FOR VOID CONTENT

MISALIGNED PLY LAMINATES

All Weights in Grams
Burn Off Temperature = 630°C (1168°F)

Fiber Density = 2.59
Resin Density = 1.26

	Laminate			9-45	12-30	13-15	13-15
1	Reference	Includes Aluminum Wire		.0239	.0242	.0245	.0204
2	Dry Weight	Includes (1)	W_D	.3514	.5768	.1362	.4570
3	Wet Weight	Includes (1)	W_W	.1878	.3130	.0992	.2445
4	Buoyancy	(2)-(3)	B	.1636	.2638	.0570	.2125
5	Weight in Air	(2)-(1)	W_A	.3275	.5526	.1117	.4366
6	Composite Density	(5)/(4)	ρ_c	2.000	2.10	1.96	2.055
7	Fiber Weight	After Burn Off	W_F	.2517	.4436	.0837	.3510
8	Resin Weight	(5)-(7)	W_R	.0758	.1090	.0280	.0856
9	Fiber Weight %	(7)/(5)x100	w_f	.769	.802	.750	.804
10	Resin Weight %	(8)/(5)x100	w_r	.231	.198	.250	.196
11	Fiber Volume %	(9)(6)/2.59	γ_f	59.3	65.0	56.8	63.8
12	Resin Volume %	(10)(6)/1.26	γ_r	33.7	33.0	39.0	31.9
13	Void Volume %	100-(11)-(12)	γ_v	7.0	2.0	4.2	4.3

TABLE 12

CALCULATIONS FOR VOID CONTENT

REFERENCE LAMINATES

All Weights in Grams
Burn Off Temperature = 800°C (1450°F)

Fiber Density = 2.61
Resin Density = 1.26

Laminate				6	6	10	10	10
1	Reference	Includes Aluminum Wire		.0284	.0284	.0212	.0284	.0284
2	Dry Weight	Includes (1)	W_D	1.1235	1.2219	.4542	.9270	.8335
3	Wet Weight	Includes (1)	W_W	.5142	.5345	.2385	.4896	.4409
4	Buoyancy	(2)-(3)	B	.6093	.6872	.2157	.4374	.3926
5	Weight in Air	(2)-(1)	W_A	1.0951	1.1933	.4330	.8986	.8051
6	Composite Density	(5)/(4)	ρ_c	1.80	1.735	2.01	2.05	2.05
7	Fiber Weight	After Burn Off	W_F	.6851	.8141	.3376	.6961	.6247
8	Resin Weight	(5)-(7)	W_R	.4100	.3992	.0954	.2025	.1804
9	Fiber Weight %	(7)/(5)x100	w_f	.626	.682	.779	.776	.775
10	Resin Weight %	(8)/(5)x100	w_r	.374	.318	.221	.224	.225
11	Fiber Volume %	(9)(6)/2.59	γ_f	43.2	45.4	60.4	61.0	60.9
12	Resin Volume	(10)(6)/1.26	γ_r	52.1	43.9	35.3	36.4	36.6
13	Void Volume %	100-(11)-(12)	γ_v	4.7	10.7	4.3	2.6	2.5

TABLE 13

CALCULATIONS FOR VOID CONTENT

MISALIGNED PLY LAMINATES

All Weights in Grams
Burn Off Temperature = 800°C (1450°F)

Fiber Density = 2.61
Resin Density = 1.26

	Laminate			9-15	9-30	9-45	12-30	13-15
1	Reference	Includes Aluminum Wire		.0212	.0212	.0212	.0212	.0212
2	Dry Weight	Includes (1)	W_D	1.0526	1.0854	.5424	.6113	.4467
3	Wet Weight	Includes (1)	W_W	.5146	.5554	.2755	.3316	.2371
4	Buoyancy	(2)-(3)	B	.5380	.530	.2669	.2797	.2096
5	Weight in Air	(2)-(1)	W_A	1.0314	1.0642	.5212	.5901	.4255
6	Composite Density	(5)/(4)	ϱ_c	1.92	2.01	1.951	2.11	2.03
7	Fiber Weight	After Burn off	W_F	.7867	.7970	.4286	.4729	.3310
8	Resin Weight	(5)-(7)	W_R	.2447	.2672	.0926	.1172	.0945
9	Fiber Weight %	(7)/(5)x100	w_f	.763	.748	.822	.800	.778
10	Resin Weight %	(8)/(5)x100	w_r	.237	.252	.178	.200	.212
11	Fiber Volume %	(9)(6)/2.59	γ_f	56.1	58.0	62.1	64.7	61.0
12	Resin Volume %	(10)(6)/1.26	γ_r	31.5	40.2	27.6	33.5	34.2
13	Void Volume %	100-(11)-(12)	γ_v	12.4	1.8	10.3	1.8	4.8

TABLE 14

SUMMARY OF CALCULATIONS FOR VOID CONTENT

Laminate	6	9-15	9-30	9-45	10	11	12-30	13-15
Average Fiber Volume %								
$\rho_f = 2.59$	45.85	58.0	62.4	59.3	58.55	61.1	65.0	60.3
$\rho_f = 2.61$	44.30	56.1	58.0	62.1	60.7	60.9	64.7	61.0
Average Resin Volume %								
$\rho_f = 2.59$	47.6	37.6	33.33	33.7	39.05	36.65	33.0	35.45
$\rho_f = 2.61$	48.0	31.5	40.2	27.6	35.85	36.6	33.5	34.2
Average Void Volume %								
$\rho_f = 2.59$	6.55	4.4	4.27	7.0	2.4	2.25	2.0	4.25
$\rho_f = 2.61$	7.7	12.4	1.8	10.3	3.45	2.5	1.8	4.8

Thesis
W283

118374

Watterson
High compressive stress, low cycle fatigue of a composite material.